Effect of Interchain Coupling on Electron-Spin Resonance in Nearly One-Dimensional Systems*

Michael J. Hennessy and Carl D. McElwee†
Department of Physics, University of Kansas, Lawrence, Kansas 66044

and

Peter M. Richards‡
Department of Physics, University of Kansas, Lawrence, Kansas 66044
and Sandia Laboratories, Albuquerque, New Mexico 87115

(Received 20 July 1972)

We present a theoretical and experimental study of the electron-spin-resonance (ESR) line shape in Heisenberg linear-chain systems which have small but non-negligible interchain coupling. Weak interchain coupling can drastically alter the characteristic one-dimensional line shape as well as produce three-dimensional ordering below a critical temperature T_N. Since T_N is observable in a majority of "linear-chain" compounds, the treatment given here has broad application to ESR and structure studies. The rate for off-chain diffusion is proportional to $J'(J'/J)^{1/3}$, where J and J' are the intra- and interchain couplings, respectively. This dependence comes from the slow rate of diffusion in one dimension. Interchain spin flips then proceed at a rate considerably faster than would be expected on the basis of an anisotropic diffusion equation or transition probabilities. As a consequence, interchain coupling can be very effective in limiting the one-dimensional divergences which produce a non-Lorentzian line. Measurements are reported in $Cu(NH_3)_4SO_4 \cdot H_2O$ (CTS), $CsMnCl_3 \cdot 2H_2O$ (CMC), and $CuCl_2 \cdot 2NC_5H_5$ (CuPC). CTS has a Lorentzian line shape out to almost 14 half-widths, which is consistent with our theory and the observed T_N. The line shape in CMC is only moderately non-Lorentzian. The value of J' required to fit the present theory to the line-shape data is between 2 and 4 times greater than estimated from the observed T_N and spin-wave spectrum in CMC. The line shape in CuPC is highly non-Lorentzian, from which we estimate $J'/J \approx 2 \times 10^{-3}$. This is in reasonable accord with a recent measurement of T_N in the compound.

I. INTRODUCTION

One-dimensional magnetic systems have been of theoretical interest at least since the classic work of Bethe[1] on the antiferromagnetic Heisenberg chain. In recent years, the interest has become considerably more than academic with the discovery of compounds which exhibit one-dimensional magnetic properties even though the crystals themselves are three dimensional. In particular, the salt $(CH_3)_4NMnCl_3$, referred to as TMMC, has been shown[2-4] to be highly one dimensional.

Experiments on TMMC and other compounds have provided detailed comparison with theories of properties which are peculiar to one dimension. Spin dynamics is one such property, and in the high-temperature region where spin diffusion is expected to characterize the motion, magnetic resonance has proved to be a very useful tool. The value of magnetic resonance stems from the fact that the linewidth and line shape in strongly exchange-coupled systems are determined by the long-time behavior of spin correlation functions such as $\langle S_i^z(t)S_j^z(0)\rangle$, where S_i^z is the z component of spin at lattice site i. If this correlation function behaves diffusively for long times t, then it is proportional to $t^{-d/2}$ for $t \to \infty$, where d is the dimensionality, as results from solution of the diffusion equation given the initial condition of only the ith spin having a nonequilibrium value at $t=0$. In one or two dimensions, there is thus a divergence as $\omega \to 0$ in the Fourier component of $\langle S_i^z(t)S_j^z(0)\rangle$ at frequency ω. This has profound consequences, particularly in one dimension where the divergence is stronger than logarithmic.

Theories of exchange-narrowed magnetic-resonance linewidth[5-7] predict the width ΔH to be proportional to the $\omega = 0$ component of certain spin correlation functions. If there is a divergence for $\omega \to 0$, then an anomalously broad line results and the line shape is non-Lorentzian (a Lorentzian shape is predicted if the $\omega = 0$ component is finite). These features have been observed[8,9] and striking agreement has thus been obtained with the theories of spin diffusion in one dimension.

The one-dimensional magnetic-resonance anomalies have previously been reported in systems for which any off-chain coupling is possibly three or more orders of magnitude smaller than the strong intrachain interaction. A more common class of "one-dimensional" compounds has measurable interchain coupling J' as determined from the observed temperature T_N at which the chains order antiferromagnetically. Although J' has a signifi-

cant effect in ultimately producing three-dimensional order, it does not alter the thermodynamics at temperatures well above T_N. Thus, it has fortunately been possible to study one-dimensional specific heats and susceptibilities in less than ideal one-dimensional compounds. Two cases in point, which we treat here, are[10,11] $Cu(NH_3)_4SO_4 \cdot H_2O$ (referred to as CTS) and $CsMnCl_3 \cdot 2H_2O$ (referred to as CMC).

It is less clear whether spin dynamics of materials with small but observable interchain coupling show the characteristic magnetic-resonance signature of a one-dimensional system in the same way that thermodynamic properties do. This paper is devoted to an investigation of the problem. We present quantitative theory for the manner in which small interchain coupling alters the one-dimensional features and give experimental results for the line shapes in CTS, CMC, and the recently studied[9,12] $CuCl_2 \cdot 2NC_5H_5$, dichlor*bis*-(pyridine)-copper (II) (referred to as CuPC).

The essential result is that one-dimensional spin dynamics significantly alter the off-chain diffusion. When this is accounted for, the linewidth and line shapes both in CMC and in CTS are reasonably well accounted for. In particular, we can understand why CTS shows a Lorentzian line shape even though the interchain coupling is quite small. This feature has previously been unexplained and the subject of some conjecture.[13–15]

We analyze the data in CuPC in a somewhat different manner. The non-Lorentzian line shape gives, by itself, indication of the size of J'; and in this way we can estimate the ordering temperature.

Another feature of this work is that we do not limit ourselves to equal coupling strengths $J_1 = J_2 = J'$ in the two directions perpendicular to the chain. The crystal structures of both CMC and CuPC suggest that $J_1 \gg J_2$ is a distinct possibility so that the interchain coupling first makes the system behave two dimensionally. Arbitrary ratios of J_1/J_2 are considered both in the line-shape theory and in the relation between T_N and the interactions J_1 and J_2. Knowledge of T_N together with the line shape can fix separate values for J_1 and J_2, and we find that $J_1/J_2 \gg 1$ gives a more reasonable fit for CMC.

The paper is organized as follows. The general formalism of exchange-narrowed line shape as developed by others is reviewed in Sec. II. The peculiar features of one dimension are stressed. Section III contains the theory of how weak interchain coupling affects the line shape. A largely physical argument is given in Sec. III A and formal details are presented in Sec. III B. Certain of the approximations in Sec. III B are discussed in the Appendix. In Sec. IV, we review the theory for calculating the ordering temperature T_N in terms of interchain coupling and extend it to the case of unequal interactions J_1 and J_2. Pertinent properties of the three compounds studied are reviewed in Sec. V. For completeness, a discussion of how dipolar interactions affect interchain coupling and T_N is contained in Sec. VI. In most cases, however, they are not important. Our techniques for measuring absorption far out in the wings of the resonance line are discussed in Sec. VII. Experimental results are presented and compared with theory in Sec. VIII. Summary and conclusions are found in Sec. IX.

II. LINE-SHAPE FORMALISM

Other authors[5–7] have shown that decay of the transverse magnetization may be approximated by

$$\phi(t) = \exp\left[\int_0^t (t-\tau)\psi(\tau)\,d\tau\right], \tag{1}$$

where

$$\psi(\tau) = \hbar^{-2}\langle[\mathcal{H}'(\tau), M_+][M_-, \mathcal{H}'(0)]\rangle / \langle M_+ M_-\rangle . \tag{2}$$

In the above $\phi(t)$ describes decay of the transverse magnetization in a frame rotating at the resonance angular frequency ω_0. The line profile at any frequency ω is then proportional to $\int_{-\infty}^{\infty} dt\,\phi(t)e^{i(\omega-\omega_0)t}$. The quantities $M_\pm$ are the usual raising and lowering operators for total transverse magnetization, angular brackets stand for thermal average, and $\mathcal{H}'$ is the perturbation—hyperfine or dipolar in our case. Time dependence is given in the interaction representation by

$$\mathcal{H}'(\tau) = e^{i\mathcal{H}_0\tau/\hbar}\mathcal{H}'e^{-i\mathcal{H}_0\tau/\hbar}, \tag{3}$$

where $\mathcal{H}_0$ is the unperturbed Hamiltonian consisting of Zeeman and exchange parts

$$\mathcal{H}_0 = \hbar\omega_0 S_z + \sum_{i,j} J_{ij}\,\vec{S}_i \cdot \vec{S}_j . \tag{4}$$

The first term in Eq. (4) is the Zeeman interaction of the z component of total spin S_z with an external field $H_0 = \omega_0/\gamma_e$ applied in the z direction. (γ_e is the electronic gyromagnetic ratio.) The second term is the Heisenberg exchange interaction between spins $\vec{S}_i$ and $\vec{S}_j$ on lattice sites i and j. The exchange Hamiltonian commutes with all components of total spin. A high-temperature approximation $\hbar\omega_0 \ll k_B T$ is implicit in (2) and the stated relation between the Fourier transform of $\phi(t)$ and the shape. The above equations have previously[8,13,15] been applied to one-dimensional systems, but it is convenient to review the results here.

We consider $\phi(t)$ in three cases.

a. No exchange or motional narrowing. Here $\psi(\tau)$ is independent of τ since there is no random modulation of $\mathcal{H}'$ (we neglect for the moment nonsecular parts of $\mathcal{H}'$ which have a simple $e^{i\omega_0 t}$ modulation due to the Zeeman interaction). Equation

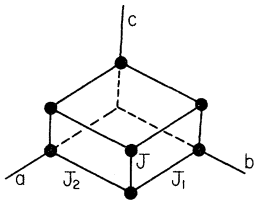

FIG. 1. Orthorhombic unit cell, defining axes and interactions as used in this paper. Chain axis is c. Interchain couplings are such that $J_1 \geq J_2$.

(1) then reduces to a Gaussian $e^{-1/2\langle\Delta\omega^2\rangle t^2}$ with $\langle\Delta\omega^2\rangle = \psi(0)$, the second moment of the resonance line.

b. Normal-exchange narrowing. Here $\psi(\tau)$ decays to a small value in a characteristic time τ_c of the order of $\hbar/J$ *and* $\int_0^\infty \psi(\tau)\,d\tau$ is finite. For $t \gg \tau_c$ an exponential dependence of $\phi(t) = e^{-\eta t}$ results with $\eta = \langle\Delta\omega^2\rangle\tau_c$. If $\langle\Delta\omega^2\rangle\tau_c \ll 1$, the decay of $\phi(t)$ is exponential over the region of experimental interest. The line is then Lorentzian except far from the center and has a half-width in angular frequency units $\eta \ll \langle\Delta\omega^2\rangle^{1/2}$.

c. Inhibited-exchange narrowing. This is the situation for the linear-chain system. The correlation function $\psi(\tau)$ decays to zero but not fast enough to guarantee convergence of $\int_0^\infty \psi(\tau)\,d\tau$. Decay of $\phi(t)$ will then be something intermediate between Gaussian and exponential. In particular, if $\psi(\tau)$ is proportional to a spin correlation function $\langle S_i^z(\tau)S_j^z\rangle$ which obeys a diffusion equation, then in one dimension we expect $\psi(\tau) \sim \tau^{-1/2}$ for $\tau \to \infty$. If we now define τ_c by

$$\psi(\tau) = \psi(0)\,(\tau_c/\tau)^{1/2} = \langle\Delta\omega^2\rangle\,(\tau_c/\tau)^{1/2} \tag{5}$$

for $\tau \gg \tau_c$, then the result of using (5) in (1) is

$$\phi(t) = e^{-(\gamma t)^{3/2}} \tag{6}$$

for $t \gg \tau_c$, with

$$\gamma = (\tfrac{4}{3})^{2/3}\,\langle\Delta\omega^2\rangle^{2/3}\tau_c^{1/3}\,. \tag{7}$$

Since we expect, once again, τ_c to be of the order of $\hbar/J$, the quantity γ/η is of the order of $\langle\Delta\omega^2\rangle^{-1/3}\tau_c^{-2/3} \sim (J/\mathcal{H}')^{2/3} \gg 1$, which expresses the ratio of the inhibited (one-dimensional) to the normal exchange-narrowed relaxation rate.

The precise value of τ_c is related to the spin-diffusion coefficient D. This quantity has been calculated by various authors[16–18] for both one and three dimensions, and will be given later.

Note that for diffusion in three dimensions $\psi(\tau)$ decays as $\tau^{-3/2}$ and normal exchange narrowing holds.[19] In two dimensions the diffusive dependence of $\psi(\tau)$ would be τ^{-1}. This results in a weak logarithmic divergence, and the ratio between inhibited and normal exchange-narrowing relaxation rates is of the order of $\ln(J/\mathcal{H}')$.

III. INTERCHAIN COUPLING AND LINE SHAPE

A. Qualitative

The manner in which weak interchain coupling alters the one-dimensional line shape is of prime importance in this paper. To avoid confusion, it is useful to establish notation at the outset. This is done with the help of Fig. 1. The c axis is always defined as the chain direction. This often, but unfortunately not always, coincides with crystallographic conventions. For example the chains in CuPC and TMMC are along the crystallographic c axis; but in CMC they are parallel to the a axis. Thus the reader should keep in mind, that for CMC, our c axis is the a axis as used in the structure determination.[20] A further source of confusion is that although the chain axis in CTS was originally[21] defined as c, in a more recent study[22] it has been taken as the a axis. The principle directions perpendicular to the chain are then taken as the a and b axes. There is in general an interaction J_1 between neighbors along the a axis and an interaction J_2 between neighbors along the b axis. We adopt the convention $J_1 \geq J_2$. It will often be convenient to discuss general features of interchain coupling without worrying about whether $J_1 \approx J_2$ or $J_1 \gg J_2$. In this case we refer to the interaction as J', with the understanding that $J' = J_1$ if $J_1 \gg J_2$. The assumption $J_1 \ll J$ is made throughout, where J is the intrachain coupling.

It is instructive at first to see, in general, how interchain coupling may or may not alter the line shape. We imagine a characteristic time t_0 beyond which three-dimensional diffusion takes over, as shown for $\psi(t)$ in Fig. 2. For times $t < t_0$, the relaxation function Eq. (1) has the one-dimensional form $e^{-(\gamma t)^{3/2}}$, since the observing time is less than that required for manifestation of the interchain effects, but for $t > t_0$ it switches to an expo-

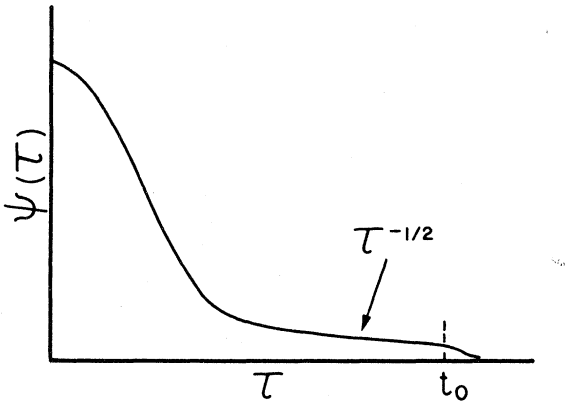

FIG. 2. Decay of autocorrelation function $\psi(\tau)$. For times $\tau > t_0$ one-dimensional $\tau^{-1/2}$ diffusion is cut off by interchain coupling.

nential $e^{-\eta t}$ with $\eta \sim \gamma^{3/2} t_0^{1/2}$, since $\int_0^t \psi(\tau)\,d\tau \approx \int_0^{t_0} \psi(\tau)\,d\tau$ for long times. The effect on line shape depends on the size of γt_0. If t_0 is sufficiently long so that $\gamma t_0 \gg 1$, the relaxation function $\phi(t)$ will have decayed to a negligibly small value by the time interchain mechanisms become important, and there will be no observable departure of the line shape or width from the one-dimensional behavior. But if $\gamma t_0 \ll 1$, $\phi(t)$ will decay exponentially throughout the region of interest and no one-dimensional anomalies are expected.

The crucial question then becomes, "what is the characteristic time t_0?" Considerations very similar to those which lead to Eq. (7) show that the rate t_0^{-1} is of the order of $(J'/\hbar)(J'/J)^{1/3}$, which is analogous to Eq. (7) if we identify $\langle \Delta\omega^2 \rangle$, of that equation, with J'^2 here. To understand qualitatively how this result comes about we regard t_0^{-1} as the characteristic rate for the spin polarization making a transition off the chain. By analogy with the treatment in Sec. II, we may define a relaxation function

$$\tilde{\phi}(t) = \exp[-\int_0^t (t-\tau)\tilde{\psi}(\tau)\,d\tau] , \tag{8}$$

which describes decay of spin polarization along the chain. That is, $\tilde{\phi}$ measures the manner in which a spin-fluctuation mode is deviated from one-dimensional motion or diffusion [a formal definition is given in Eq. (21)], and t_0^{-1} is thus given by the characteristic decay rate of $\tilde{\phi}$. The function $\tilde{\psi}(\tau)$ is related to J' by

$$\tilde{\psi}(\tau) \sim (J'/\hbar)^2 g(\tau) , \tag{9}$$

where $g(0) = 1$ and time dependence of $g(\tau)$ is governed by the unperturbed motion which in this case is diffusion in one dimension. Hence we have cast the problem of interchain-transition rate into the standard form for relaxation by a perturbation J'. Now the argument proceeds exactly as for the three cases presented in Sec. II. If $g(\tau)$ is constant in time, corresponding to no interruption of the off-chain motion by intrachain spin flips, then $t_0^{-1} \sim J'/\hbar$. If $g(\tau)$ decays in a time of the order of $\hbar/J$ and sufficiently rapidly that $\int_0^\infty g(\tau)\,d\tau$ converges, then we have the usual narrowing result $t_0^{-1} \sim (J'/\hbar)(J'/J)$. For diffusion in one dimension, though, we expect $g(\tau) \sim (\hbar\tau/J)^{-1/2}$ for long times, and thus the characteristic rate would be $t_0^{-1} \sim (J'/\hbar)(J'/J)^{1/3}$, by reasoning identical to that used in arriving at Eqs. (6) and (7).

The result $t_0^{-1} \sim (J'/\hbar)(J'/J)$ had been used previously[13,14] and was based on the assumption that interchain-coupling effects could be described by an anisotropic diffusion equation

$$\frac{\partial \rho}{\partial t} = D \frac{\partial^2 \rho}{\partial z^2} + D' \left(\frac{\partial^2 \rho}{\partial x^2} + \frac{\partial^2 \rho}{\partial y^2} \right) . \tag{10}$$

The off-chain diffusion coefficient D' could then be estimated from moments of the spin correlation functions in the usual way[16–18] as

$$D' \propto \lim_{q \to 0} (\langle \omega_q^2 \rangle^{3/2} / \langle \omega_q^4 \rangle^{1/2}) 1/q_x^2 , \tag{11}$$

where the constant of proportionality is of the order of unity and where $\langle \omega_q^n \rangle$ is the nth moment of the spectral density of $\sum_{ij} \langle S_i^z(t) S_j^z \rangle e^{i\vec{q}\cdot\vec{r}_{ij}}$. Examination of the high-temperature moments[23] then shows that $D' \sim (J'^2/\hbar J)a^2$ for $J' \ll J$, in agreement with the above remark.

The error in the reasoning of the above paragraph, based on anisotropic diffusion, is that the one-dimensional correlations do not decay rapidly enough to allow one to apply the conventional random modulation or Golden Rule approaches to calculation of the rate t_0^{-1}. Also, as we show below, the correlation $\langle S_i^z(t) S_j^z \rangle$ does not decay as $t^{-3/2}$ for $t \gg t_0$, as would be expected from Eq. (10). Instead, we find a more rapid t^{-2} decay so that, for $J' \ll J$, the characteristic time dependence of three-dimensional diffusion is not realized.

Since $J' \ll J$, there is a big difference between $t_0^{-1} \sim (J'/\hbar)(J'/J)$ and $t_0^{-1} \sim (J'/\hbar)(J'/J)^{1/3}$. The former estimate gives $\gamma t_0 \gtrsim 1$ for CTS and thus predicts a decidedly non-Lorentzian line shape in that material. The latter results in $\gamma t_0 \ll 1$ for CTS and thus a Lorentzian line, which is in agreement with experiment.

B. Quantitative

In this subsection we give more formal justification for the previous remarks about interchain effects and derive an expression for the resulting line shape.

We wish to calculate the wave-vector-dependent time-correlation function $\langle S_q^z(t) S_{-q}^z(0) \rangle$, where

$$S_q^z = N^{-1/2} \sum_j S_j^z e^{i\vec{q}\cdot\vec{r}_j} \tag{12}$$

and

$$S_q^z(t) = e^{i\mathcal{H}_0 t/\hbar} S_q^z e^{-i\mathcal{H}_0 t/\hbar} , \tag{13}$$

with $\mathcal{H}_0$ given by the fully three-dimensional Heisenberg plus Zeeman Hamiltonian of Eq. (4). Since the Zeeman term commutes with $\mathcal{H}_0$ and with S_q^z it may henceforth be neglected. We then write

$$\mathcal{H}_0 = \mathcal{H}_C + \mathcal{H}_I , \tag{14}$$

in which

$$\mathcal{H}_C = 2J \sum_i \vec{S}_i \cdot \vec{S}_{i+1} \tag{15}$$

is the Hamiltonian describing a set of independent linear chains ($\vec{r}_{i+1} \equiv \vec{r}_i + c\hat{z}$, where $\hat{z}$ is a unit vector along the chain axis and c is the nearest-neighbor intrachain spacing), and the perturbation

$$\mathcal{H}_I = \sum_{ij} G_{ij} \vec{S}_i \cdot \vec{S}_j \tag{16}$$

gives the interchain coupling ($G_{ij}=0$ if i and j are on the same chain, and $G_{ij}=J_{ij}$ otherwise). An interaction representation[7] is introduced whereby

$$S_q^z(t)=e^{i\mathcal{H}_C t/\hbar}\,\tilde{S}_q^z(t)e^{-i\mathcal{H}_C t/\hbar}\ . \tag{17}$$

We assume sufficiently high temperature that $\mathcal{H}_I$ has no effect on the thermodynamic properties. Then $\mathcal{H}_C$ may be commuted through the density matrix in the calculation of the thermal average $\langle S_q^z(t)S_{-q}^z(0)\rangle$ so that

$$\langle S_q^z(t)S_{-q}^z(0)\rangle=\langle \tilde{S}_q^z(t)\bar{S}_{-q}^z(-t)\rangle\ , \tag{18}$$

where, for any operator $\mathcal{O}$,

$$\bar{\mathcal{O}}(t)=e^{i\mathcal{H}_C t/\hbar}\,\mathcal{O}(0)e^{-i\mathcal{H}_C t/\hbar} \tag{19}$$

has a time dependence given strictly by the intrachain Hamiltonian. The equation of motion for $\tilde{S}_q^z(t)$ is

$$\frac{d}{dt}\tilde{S}_q^z(t)=\frac{i}{\hbar}\,[\bar{\mathcal{H}}_I(-t),\tilde{S}_q^z(t)]\ . \tag{20}$$

The correlation of $\tilde{S}_q^z(t)$ is defined in terms of a relaxation function $\tilde{\phi}_q(t)$ by

$$\langle\tilde{S}_q^z(t)\bar{S}_{-q}^z(0)\rangle=\langle S_q^z S_{-q}^z\rangle\tilde{\varphi}_q(t)\ . \tag{21}$$

We then assume that Eq. (18) may be reduced to

$$\begin{aligned}\langle S_q^z(t)S_{-q}^z(0)\rangle&=\langle\bar{S}_q^z(t)\bar{S}_{-q}^z(-t)\rangle\\&=\langle S_q^z(0)\bar{S}_{-q}^z(-t)\rangle\tilde{\phi}_q(t)\ ,\end{aligned} \tag{22}$$

which is equivalent to replacing $\tilde{S}_q^z(t)$ by $S_q^z(0)\tilde{\phi}_q(t)$. This approximation has the advantage of leading to a form in which $\langle S_q^z(t)S_{-q}^z(0)\rangle$ is a simple product of the unperturbed (linear-chain) relaxation function and a relaxation function governed by interchain effects. It is an approximation in the sense that it neglects correlations between derivatives of $\tilde{S}_q^z(t)$ and of $\bar{S}_q^z(t)$. However, it is correct to order t^2 in the high-temperature limit and thus preserves the second moment, as shown in the Appendix.

The equation of motion (20) is iterated in the standard way,[5-7] and thus we obtain in the long-time–short-time approximation

$$\tilde{\phi}_q(t)=\exp\Big[-\int_0^t(t-\tau)\tilde{\psi}_q(\tau)\,d\tau\Big]\ , \tag{23}$$

where

$$\tilde{\psi}_q(\tau)=\hbar^{-2}\,\langle[\bar{\mathcal{H}}_I(\tau),[\mathcal{H}_I,S_q^z]\,]S_{-q}^z\rangle/\langle S_q^z S_{-q}^z\rangle\ . \tag{24}$$

In the high-temperature limit, the factors may be rearranged to yield the more convenient form

$$\tilde{\psi}_q(\tau)=\hbar^{-2}\,\langle\bar{\mathcal{H}}_I(\tau)[\,[\mathcal{H}_I,S_q^z],S_{-q}^z\,]\rangle/\langle S_q^z S_{-q}^z\rangle\ , \tag{25}$$

which may then be expressed in terms of spin time-correlation functions. The steps used in going from (20) to (21) and (24) are the same as used in deriving the fundamental Eq. (1).

Evaluation of the commutator in Eq. (25) together with Eq. (16) then yields

$$\begin{aligned}\tilde{\psi}_q(\tau)=&\frac{12}{S(S+1)}\,N^{-1}\\&\times\sum_{q'}\langle\bar{S}_{q'}^z(\tau)S_{-q'}^z(0)\rangle^2\,|G_{q'}-G_{q'-q}|^2\ ,\end{aligned} \tag{26}$$

where

$$G_q=\sum_j G_{ij}e^{i\vec{q}\cdot\vec{r}_{ij}}\ .$$

Because of the interchain nature of $\mathcal{H}_I$, the four-spin correlation functions such as

$$\langle\bar{S}_i^+(\tau)\bar{S}_j^-(\tau)S_k^+(0)S_l^-(0)\rangle\ ,$$

which result from Eq. (25), are such that i, j, k, and l cannot belong to the same chain. Hence, the decoupling implied by $\langle S_{q'}^{-z}(\tau)S_{-q'}^z(0)\rangle^2$ in Eq. (26) is exact here. The quantities $S_i^\pm$ are the usual raising and lowering operators, and isotropy $[\langle\bar{S}_i^+(\tau)S_j^-(0)\rangle=2\,\langle\bar{S}_i^z(\tau)S_j^z(0)\rangle\,]$ has been assumed.

For the orthorhombic lattice of Fig. 1, we have

$$G_q=2J_1\cos q_x a+2J_2\cos q_y b\ . \tag{27}$$

We take the diffusion limit

$$\langle\bar{S}_q^z(\tau)S_{-q}^z(0)\rangle=\tfrac{1}{3}\,S(S+1)e^{-Dq_z^2\tau} \tag{28}$$

appropriate to high temperature and small q_z. Since G_q depends only on q_x and q_y and $\langle\bar{S}_q^z(\tau)S_{-q}^z(0)\rangle$ depends only on q_z, the summation in (26) is readily performed upon converting it to a three-dimensional integral over the first Brillouin zone of an orthorhombic lattice. The final result is

$$\begin{aligned}\tilde{\psi}_q(\tau)=&\frac{8}{3}\,\frac{S(S+1)}{\pi^{1/2}}\left(\frac{1}{2D\tau/c^2}\right)^{1/2}\\&\times[J_1^2(1-\cos q_x a)+J_2^2(1-\cos q_y b)]\end{aligned} \tag{29}$$

for $D\tau(\pi^2/c^2)\gg 1$, so that the upper limits of the q_z integral may be extended to $\pm\infty$. The $\tau^{-1/2}$ dependence is expected from the qualitative arguments of Sec. III A.

The relaxation function $\tilde{\phi}_q(\tau)$ is obtained by performing the integration required in Eq. (23) with $\tilde{\psi}_q(\tau)$ given by Eq. (29). We have, in terms of dimensionless variables

$$\tilde{\phi}_q(\tau)=\exp\{-(\tau/t_0)^{3/2}[1-\cos q_x a+\alpha^2(1-\cos q_y a)]\}\ , \tag{30}$$

where

$$t_0=\left(\frac{9}{32S(S+1)}\right)^{2/3}\left(\frac{2\pi D}{c^2}\right)^{1/3}\left(\frac{J_1}{\hbar}\right)^{-4/3} \tag{31}$$

and

$$\alpha=J_2/J_1\ . \tag{32}$$

Equation (31) gives formal definition of the characteristic time t_0. Since D/c^2 is proportional to J, this definition is consistent with the predicted dependence $t_0^{-1}\propto J_1(J_1/J)^{1/3}$ based on the qualitative arguments of Sec. III A.

The final desired result from Eqs. (22) and (28) is

$$\langle S_q^z(\tau)S_{-q}^z\rangle = \tfrac{1}{3}S(S+1)e^{-Dq_z^2\tau}\tilde{\phi}_q(\tau)\,, \tag{33}$$

with $\tilde{\phi}_q(t)$ given by Eq. (30). We must now relate $\langle S_q^z(\tau)S_{-q}^z\rangle$ to the function $\psi(\tau)$ which, from Eq. (1), describes the ESR line shape. For most systems of interest the secular part of the dipolar interaction dominates, and this gives

$$\psi_d(\tau) = \frac{27}{8}\frac{\gamma_e^4\hbar^2N^{-2}}{S(S+1)}\sum_{ijkl} r_{ij}^{-3}r_{kl}^{-3}(1-3\cos^2\theta_{ij}) \times (1-3\cos^2\theta_{kl})\langle S_i^z(\tau)S_j^+(\tau)S_k^z(0)S_l^-(0)\rangle\,, \tag{34}$$

where the subscript d denotes the dipolar contribution, γ_e is the electronic gyromagnetic ratio, and θ_{ij} is the angle between $\vec{r}_{ij}$ and the applied field. The nonsecular ($\Delta M = \pm 1, \pm 2$, where ΔM is the change in magnetic quantum number) terms do not contribute to one-dimensional anomalies since they contain Zeeman-frequency modulation factors which remove the divergence of $\int_0^\infty \psi(\tau)\,d\tau$. This point is discussed in Refs. 8 and 15.

Decoupling the four-spin correlation function in Eq. (34) then leads to

$$\psi_d(\tau) = \frac{27}{4}\frac{\gamma_e^4\hbar^2N^{-1}}{S(S+1)}\sum_q |F_q|^2\langle S_q^z(\tau)S_{-q}^z\rangle^2\,, \tag{35}$$

where

$$F_q = \sum_j r_{ij}^{-3}(1-3\cos^2\theta_{ij})e^{-i\vec{q}\cdot\vec{r}_{ij}}\,. \tag{36}$$

Note that the decoupling employed here is not exact, as it is in Eq. (26), since all spins can belong to the same chain.

In the neglect of interchain-dipolar interactions, we have simply

$$F_q \approx 2(1-3\cos^2\theta)c^{-3}\cos q_z c\,, \tag{37}$$

where z is the chain axis, which makes an angle θ with respect to the applied field. Since $Dt(\pi^2/c^2) \gg 1$ for times of interest, we may further take $\cos q_z c \approx 1$ for values of q_z which contribute appreciably to the sum in Eq. (35). As a result of these simplifications, we find that $\psi_d(\tau)$ is proportional to $\sum_q \langle S_q^z(\tau)S_{-q}^z\rangle^2$, so that upon using Eq. (33), we have

$$\psi_d(\tau) = \psi_d(0)\frac{abc}{8\pi^3}\int_{-\pi/c}^{\pi/c} dq_z\, e^{-2Dq_z^2\tau}\int_{-\pi/a}^{\pi/a} dq_x \times \int_{-\pi/b}^{\pi/b} dq_y\,[\tilde{\phi}_q(\tau)]^2 \tag{38}$$

after converting the summation to an integral. The integrations may be performed exactly with $\tilde{\phi}_q(\tau)$ given by (30). The result is

$$\psi_d(\tau) = \frac{\psi_d(0)}{2\pi^{1/2}}\left(\frac{c^2}{2D\tau}\right)^{1/2} e^{-2(1+\alpha^2)(\tau/t_0)^{3/2}} \times I_0(2(\tau/t_0)^{3/2})I_0(2\alpha^2(\tau/t_0)^{3/2})\,, \tag{39}$$

where t_0 and α are defined in Eqs. (31) and (32) and where I_0 is the zeroth-order Bessel function of imaginary argument. The assumption $D\tau(\pi^2/c^2) \gg 1$ has been made so that the upper limit of the q_z integral may be extended to infinity.

For $\tau \ll t_0$, the Bessel functions and the exponential are unity so that $\psi_d(\tau)$ is proportional to $\tau^{-1/2}$, the one-dimensional diffusion result. For $\tau \gg t_0$ and $\alpha^{4/3} \gg t_0$, the asymptotic expansion[24] $I_0(z) \approx e^z/(2\pi z)^{1/2}$ may be used to show that $\psi_d(\tau) \propto \tau^{-2}$; whereas three-dimensional diffusion—even anisotropic as in Eq. (10)—gives a $\tau^{-3/2}$ decay for $\tau \to \infty$. If J_1 is much greater than J_2, so that $\alpha \ll 1$, there is a region for which $\tau_0 \ll \tau \ll \alpha^{-4/3}t_0$. Here the decay is proportional to $\tau^{-5/4} = \tau^{-1/2}\tau^{-3/4}$ since only J_1 is effective in producing off-chain motion.

Equation (39) may be used in Eq. (1) to obtain the relaxation function $\phi(t)$. We show the related quantity $\int_0^t (t-\tau)\psi_d(\tau)\,d\tau/t^{3/2}$ in Fig. 3 for two values $\alpha = 1$ and $\alpha = 10^{-2}$. A change from $\phi(t)$ decaying as $e^{-t^{3/2}}$ to the slower e^{-t} is seen, as expected, for $t \gtrsim t_0$. Specific computed line shapes from Eqs. (39) and (1) are shown along with the experimental data in Sec. VIII.

IV. INTERCHAIN COUPLING AND T_N

A one-dimensional system with short-range interactions can have no long-range order at finite temperature. Hence, any ordering effects must be attributed to interchain coupling, and the value of the transition temperature T_N can tell something about the strength of J'. The most reliable estimates of T_N in terms of J' probably come from random-phase approximation (RPA) and other Green's-function schemes. These may be put in the form

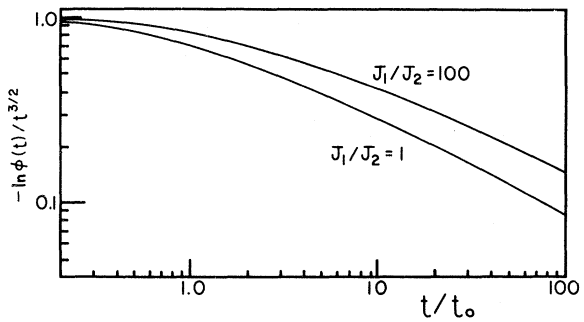

FIG. 3. Logarithm of relaxation function divided by $t^{3/2}$. Here $-\ln\varphi(t) = \int_0^t (t-\tau)\,\psi_d(\tau)\,d\tau$ and is normalized so that $-\ln\varphi(t)/t^{3/2} = 1$ for $t \to 0$. The dipolar correlation function $\psi_d(\tau)$ is given by Eq. (39) and the characteristic time t_0 by Eq. (31). The curves give an asymptotic $t^{-1/2}$ dependence, which means $-\ln\varphi(t) \propto t$, i.e., an exponential decay.

$$k_B T_N/J = \tfrac{4}{3} S(S+1) f/I \,, \tag{40}$$

where

$$I = N^{-1} \sum_q [1 - J(q)/J(0)]^{-1} \,, \tag{41}$$

in which $J(q) = \sum_j J_{ij}\, e^{-i\vec{q}\cdot\vec{r}_{ij}}$. The quantity f is a factor which depends on the decoupling and is given by $f = 1$ for RPA, $f = 1 + [(S+1)/3S][(I-1)/I]$ for Callen decoupling[25] and $f = 1 + [(S-1)/3S][(I-1)/I]$ as suggested by Tahir-Kheli[26] to obtain agreement with Padè approximates for the critical temperature in cubic ferromagnets. Green's-function theories predict the same transition temperature for ferromagnetic and for antiferromagnetic interactions, which are rigorously correct for classical spins. Rushbrooke and Wood[27] have shown there is about a 13% difference between antiferromagnetic and ferromagnetic transition temperatures for spin-$\frac{1}{2}$ and simple-cubic lattice. The difference drops to 1.3% for spin-$\frac{5}{2}$. Thus, there should not be a serious error in applying, for example, the Tahir-Kheli values of f to an antiferromagnet.

The integral I has been obtained analytically by Montroll[28] for the case $J_1 = J_2$. Independently, Oguchi[29] calculated it numerically for $J_1 = J_2$ and made the original estimate $J_1 \approx 10^{-2} J$ for CTS with $f = 1$ and the then known figure for T_N. For arbitrary values of J_1 and J_2, we have

$$I = \frac{1}{\pi^3} \int\int\int_{-\pi}^{\pi} \frac{dx\, dy\, dz}{1 - \cos z + \alpha_1(1-\cos x) + \alpha_2(1-\cos y)} \,, \tag{42}$$

where $\alpha_{1,2} = J_{1,2}/J \ll 1$. As shown by Montroll, this can be converted to

$$I = \int_0^\infty du\, e^{-(1+\alpha_1+\alpha_2)u} I_0(\alpha_1 u) I_0(\alpha_2 u) I_0(u) \,, \tag{43}$$

which can then be integrated numerically for arbitrary α_1 and α_2. We have done this and found

$$I = 0.64 (J/J_1)^{1/2} [1 + 0.253 \ln(J_1/J_2)] \tag{44}$$

for $J/J_1 \gg 1$ and $J_1/J_2 \geq 1$.

Equation (44) can then be used together with Eq. (40) to determine J_1 and J_2 for any observed value of $k_B T_N/J$.

V. PROPERTIES OF CTS, CMC, AND CuPC

We review below the evidence for linear-chain behavior in the specific compounds studied. Crystal structures, estimated linewidths and, where possible, magnitudes of interchain coupling are also considered.

A. CTS

The specific heat[30] and susceptibility[31] of CTS have been shown by Griffiths[10] to conform to those of a spin-$\frac{1}{2}$ linear chain with $J/k_B = 3.15$ K. Antiferromagnetic ordering[32] occurs at a temperature $T_N = 0.43$ K.

The pertinent crystal structure as viewed along the chain axis is given in Fig. 4. We show only those ligands which are the most likely to take part in interchain coupling by superexchange along hydrogen-bond paths.[22] From the figure, we note that the distances Cu_1–Cu_2 and Cu_2–Cu_4 are approximately equal. Also the segments of the Cu–N–O–N–Cu paths are about the same for Cu_1–Cu_2, Cu_2–Cu_4, and Cu_2–Cu_3 coupling. Hence, a simple two-dimensional structure which is perhaps most applicable to interchain coupling in CTS is a triangular lattice, rather than a rectangular one. The triangular lattice with equal coupling $J'(6)$ to six nearest neighbors should not give much different results than the square lattice with equal coupling $J'(4)$ to four nearest neighbors. We can estimate the effect on the characteristic time t_0 as follows. Assume, consistent with the integrand in Eq. (42) for small q, that T_N is a function of $ZJ'(Z)$ where Z is the number of interchain neighbors. Then we have

$$J'(6) = \tfrac{4}{6} J'(4) \,, \tag{45}$$

where $J'(6)$ and $J'(4)$ are, respectively, estimates of J' for a triangular and square lattice with the same T_N. From Eqs. (26) and (29) we can deduce that

$$t_0^{-1} \propto \{Z[J'(Z)]^2\}^{2/3} \tag{46}$$

should be approximately correct. Hence by combining (45) and (46), we see that

$$t_0(6)/t_0(4) = (\tfrac{3}{2})^{2/3} = 1.3 \,, \tag{47}$$

where $t_0(6)$ and $t_0(4)$ are, respectively, the characteristic times for triangular and for square lattices, given the same intrachain coupling J and Néel temperature T_N. (By referring to triangular and square lattices we mean, of course, only that portion of the three-dimensional lattice which describes planes perpendicular to the chain.)

Since Eq. (47) shows that there is likely to be only a 30% difference in t_0 between assuming a square or a triangular lattice, we approximate CTS by the square lattice for convenience. The important point is that the structure suggests a fully two-dimensional (roughly equal couplings in the x and y directions) interchain coupling. Whether the coordination number is 4 or 6 is of relatively minor consequence.

Values of $J_1 = J_2 = J'$ are given in Table I for the various choices of f discussed after Eq. (41). As mentioned above, equal coupling to four nearest neighbors is assumed. The quantity t_0, defined in Eq. (31) gives the time at which the decay ceases to be characterized by one dimensional diffusion. It is determined from J_1 once D is known. Here we take the Tahir-Kheli and McFadden result[18]

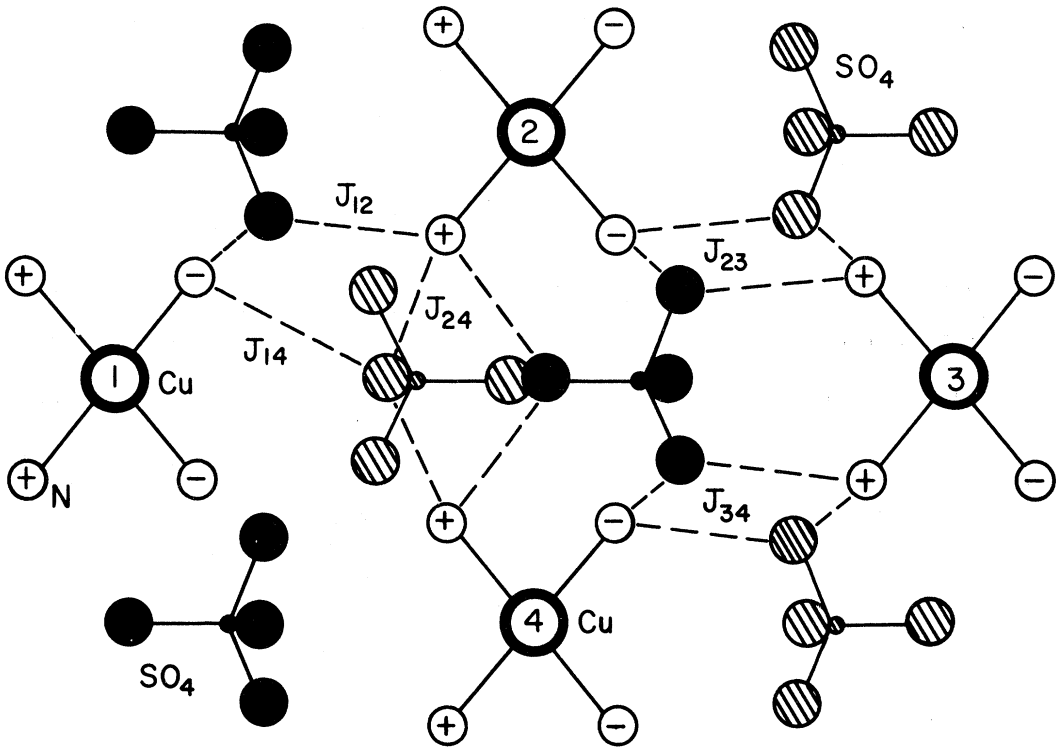

FIG. 4. Structure of $Cu(NH_3)_4SO_4 \cdot H_2O$ viewed along chain axis. Cu ions are shown in one plane only. Darkened sulfate groups lie above the plane, lightly shaded ones lie below the plane. Nitrogens with "+" are above the plane, those with "−" are below the plane. Only a few of the several N–O paths in the likely Cu–N–O–N–Cu superexchange linkages are shown, as indicated by dashed lines. They contribute to Cu–Cu interactions J_{ij} as indicated. By symmetry $J_{23}=J_{34}$ and $J_{14}=J_{12}$, but $J_{14}\neq J_{23}$ in general since there is not a mirror plane between 2 and 4. Plus (+) and minus (−) signs on nitrogens are reversed in plane immediately above and below the one shown. N–O distances for superexchange (and hydrogen bonding) paths vary between 2.978 and 3.183 Å (Ref. 22). Cu–Cu distances are $r_{12}=r_{14}=r_{23}=r_{34}=6.958$ Å, $r_{24}=7.069$ Å. Not shown are H_2O molecules, through which intrachain superexchange is believed to take place.

$$D=\pi^{1/2}Jc^2/\hbar \tag{48}$$

for spin-$\frac{1}{2}$. Use of (48) in (31) then leads to values of t_0 shown in Table II.

The relaxation rate γ is related to the ideal one-dimensional half-width at half-maximum $\Delta\tilde{H}_{1/2}$ by

$$\gamma=\gamma_e\Delta\tilde{H}_{1/2}/1.44\ , \tag{49}$$

where γ_e is the electronic gyromagnetic ratio and the factor of 1.44 comes from the $e^{-(\gamma t)^{3/2}}$ decay. (The factor would be 1 for a Lorentzian line and 1.67 for a Gaussian.) The width $\Delta\tilde{H}_{1/2}$ is equal to the *observed* width $\Delta H_{1/2}$ only in the absence of interchain effects. Its calculation is subject to several uncertainties. Equations (1), (35), (36), and (39) predict a full dipolar width $2\Delta\tilde{H}_{1/2}=135$ Oe for the field H applied along the chain axis. Included in this figure is an 11% contribution to F_q from interchain-dipolar coupling. However, the same equations overestimate the width in TMMC by about a factor of 1.7, and we expect $\Delta\tilde{H}_{1/2}=\Delta H_{1/2}$ for TMMC. Dividing by a factor of 1.7 then reduces the one-dimensional dipolar width to 80 Oe, which is tantamount to scaling the width in CTS to the observed width in TMMC—taking account of the different spin values, J's, and lattice constants.

Recently,[9] the salt *bis*-(*N*-methylsalicylaldimin-

TABLE I. Intrachain coupling J and Néel temperature T_N for CTS, CMC, CuPC. From these numbers estimates are shown for interchain coupling based on random-phase-approximation (RPA), Callen (C), and Tahir-Kheli (TK) methods. For CTS and CuPC figures are only for $J_1=J_2$, while we also consider $J_1=10J_2$ and $J_1=100J_2$ for CMC. [See Eq. (44) and accompanying text.]

	$Cu(NH_3)_4SO_4 \cdot H_2O$ (CTS)	$CsMnCl_3 \cdot 2H_2O$ (CMC)	$CuCl_2 \cdot 2NC_5H_5$ (CuPC)
J/k_B	3.15 K	3.0 K	13.6 K
T_N	0.43 K	4.89 K	1.135 K
$J_1=J_2$			
J_1/J (RPA)	7.6×10^{-3}	7.9×10^{-3}	2.8×10^{-3}
J_1/J (C)	2.2×10^{-3}	4.1×10^{-3}	1.5×10^{-3}
J_1/J (TK)	1.5×10^{-2}	5.8×10^{-3}	5.7×10^{-3}
$J_1=10J_2$			
J_1/J (TK)		1.5×10^{-2}	
$J_1=100J_2$			
J_1/J (TK)		2.6×10^{-2}	

TABLE II. Experimental and theoretical linewidths in CTS and CMC.

	$2\Delta H_{1/2}$ (expt)[a]	$2\Delta\tilde{H}_{1/2}$ (theory)		t_0 (sec)[b]	γt_0[c]	$2\Delta H_{1/2}$ (theory) (Oe)
CTS	40 Oe	75 Oe[d]	$J_1=J_2$, RPA	1.8×10^{-9}	0.8	43
			$J_1=J_2$, C	9.6×10^{-9}	4.3	72
			$J_1=J_2$, TK	6.9×10^{-10}	0.32	28
CMC	230 Oe	490 Oe[e]	$J_1=J_2$, RPA	4.9×10^{-10}	1.5	340
			$J_1=J_2$, C	1.2×10^{-9}	3.5	
			$J_1=J_2$, TK	7.5×10^{-10}	2.2	370
			$J_1=10J_2$, TK	2.1×10^{-10}	0.64	306
			$J_1=100J_2$, TK	1.0×10^{-10}	0.32	240

[a]This work, field parallel to chain axis. Room temperature, 8.68 GHz.
[b]Obtained from Eq. (31) and values of J_1 given in Table I.
[c]γ is the decay constant for the pure one-dimensional relaxation function $e^{-(\gamma t)^{3/2}}$. It is related to $\Delta\tilde{H}_{1/2}$ by $\gamma=\gamma_e\Delta H_{1/2}$ 1.44, where $2\Delta\tilde{H}_{1/2}$ is the theoretical full width in the absence of interchain coupling. ($\gamma_e=1.76\times10^7$ sec^{-1} G^{-1} is the gyromagnetic ratio for free-electron spins.)
[d]Chosen to give near-Lorentzian line for Tahir-Kheli (TK) value of J_1/J.
[e]Obtained by scaling with observed width in TMMC.

ato)-copper (referred to as CuNSAL) has been shown to have a one-dimensional line shape. The structure of CuNSAL also suggests that it should be as nearly a one-dimensional system as is TMMC. Since it has the same spin and J value[9] as CTS, it would seem most reasonable to predict the width of CTS by scaling to that observed in CuNSAL. We have[9] $2\Delta H_{1/2}=240$ Oe in CuNSAL, and the interchain distances in CTS and CuNSAL are in the ratio 5.33/3.33. This method then predicts $2\Delta\tilde{H}_{1/2}=37$ Oe—since $\Delta\tilde{H}_{1/2}$ scales as c^{-4}—which is nearly equal to the observed width. However, $\Delta\tilde{H}_{1/2}\approx\Delta H_{1/2}$ should not be correct for CTS since a Lorentzian line is observed.

A further complication is the large hyperfine coupling in CTS. Rogers[33] has deduced a hyperfine constant $A_{\parallel}=0.02$ cm^{-1} from ESR studies of the $Cu(NH_3)_4^{++}$ complex in a glass matrix, where the subscript $\parallel$ is for the component parallel to the tetramine axis. This converts to a predicted one-dimensional linewidth $2\Delta\tilde{H}_{1/2}=53$ Oe due to hyperfine coupling alone.[13]

Thus there appears to be considerable latitude in the "reasonable" values one might assign to γ. A possible source of the difficulty may be nondipolar interactions such as anisotropic exchange which could be prevalent for the non-S-state Cu^{++} ion. We have taken $\gamma=4.5\times10^8$ sec^{-1}, which corresponds to $2\Delta\tilde{H}_{1/2}=75$ Oe. This choice is motivated by the fact that it is about the largest value of γ which can give a Lorentzian line of the observed width $2\Delta H_{1/2}=40$ Oe for any J_1 shown in Table I. The resulting products γt_0 are given in Table II along with the predicted linewidths.

B. CMC

The susceptibility of spin-$\frac{5}{2}$ CMC has been measured by Smith and Friedberg[11] who obtained $J/k_B=3.0$ K by comparison with Fisher's[34] exact results for the classical-spin Heisenberg antiferromagnet and with interpolations for large, finite spin. Antiferromagnetic ordering[35,36] occurs at $T_N=4.89$ K.

The structure viewed along the chain axis is shown in Fig. 5. The lattice of magnetic ions is orthorhombic apart from a small zig-zag of the chains which we ignore so that the theory of Secs. III and IV may be applied directly. It is probable that $J_1\gg J_2$, as may be seen from the distances given in the figure. The interchain-superexchange linkage is likely to be Mn–O–Cl–Mn for both J_1 and J_2. A simple r^{-10} dependence[37] of $J_{1,2}$ upon Mn–Mn separation r would then predict $J_1/J_2=11$. Estimates of J_1 for various ratios J_1/J_2 are presented in Table I, where use has been made of Eq. (44) to obtain J_1 for a particular value of J_1/J_2.

The Tahir-Kheli and McFadden diffusion constant

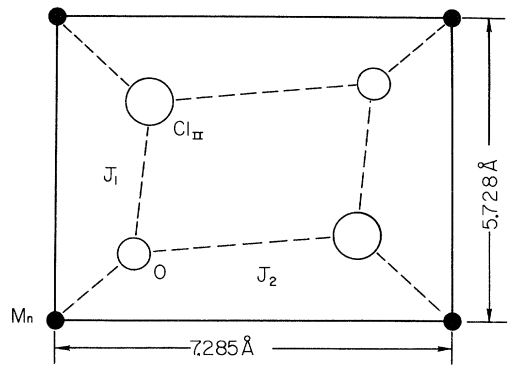

FIG. 5. Representation of $CsMnCl_3\cdot2H_2O$ (CMC). View is projection onto a plane perpendicular to the chain axis. Probable superexchange paths for interchain couplings J_1 and J_2 are shown.

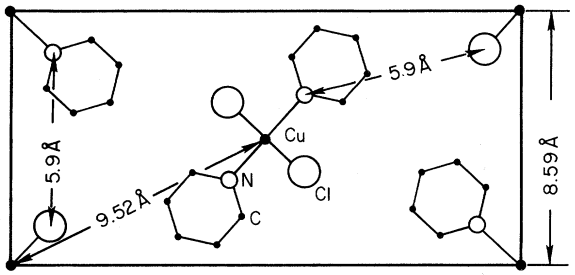

FIG. 6. Structure of $CuCl_2 \cdot 2NC_5H_5$ (CuPC) viewed along chain axis. Cu–Cu distances and N–Cl part of likely superexchange paths are shown.

is $D = 4.34\ Jc^2/\hbar$ for spin $S = \frac{5}{2}$. This number is used in Eq. (31) to arrive at the figures for t_0 in Table II.

Skalyo *et al.*[38] have done neutron scattering below the ordering temperature and find $J_1 + J_2 = 6.8 \times 10^{-3} J$ (J_1, J_2, and J are in our notation, which differs from theirs) from the spin-wave spectrum for $q_z = 0$. The estimates in Table I all give higher figures for $J_1 + J_2$, but they are of the same order of magnitude.

The relaxation rate is determined by scaling with the observed width in TMMC, which is $2\Delta H_{1/2} = 1360$ Oe for the field along the chain axis. Since CMC and TMMC have the same spin and have S-state magnetic ions, for which classical-dipolar coupling should be valid, this appears to be a reasonable procedure. Furthermore, hyperfine coupling is unimportant for Mn^{++} ESR widths because the large spin-$\frac{5}{2}$ gives greatly added weight to the dipolar term. Thus, for CMC, there should not be the uncertainties associated with estimating the CTS width. We then have $2\Delta\tilde{H}_{1/2} = 1360(3.25/4.53)^4(3/7)^{1/3} = 490$ Oe for CMC, upon using 3.25 and 4.53 Å as the intrachain distances in TMMC and CMC, respectively, and taking $J/k_B = 7$ K as a representative value[2–4] for TMMC. The resulting values for t_0 are given in Table II.

C. CuPC

The susceptibility[12] of CuPC has been measured down to 1.3 K and fits that of a spin-$\frac{1}{2}$ Heisenberg chain with $J/k_B = 13.6$ K. Specific-heat data[12] down to 2.0 K give $J/k_B = 11.5$ K. No ordering transition has yet been reported in the literature; however, very recent specific-heat measurements by Duffy[39] and Strandburg indicate that $T_N = 1.135$ K. The structure viewed along the chain is presented in Fig. 6 and is suggestive of $J_1 \approx 3J_2$ based on an r^{-10} dependence as discussed for CMC.

This work was completed before we were aware of the value[39] of T_N in CuPC. We therefore adapted a different analysis technique than used for CTS and CMC. In those materials we predicted line shapes from the observed Néel temperatures. For CuPC we used the line shape as previously reported[9] and reproduced in this paper to estimate T_N. This analysis is presented in Sec. VIII. Because of the aforementioned difficulties with Cu^{++} in CTS, it is hard to give a meaningful prediction for $2\Delta\tilde{H}_{1/2}$. We do note, though, that scaling with the observed width in CuNSAL gives $2\Delta\tilde{H}_{1/2} = 80$ Oe, which agrees well with experiment (see Sec. VIII).

VI. INTERCHAIN-DIPOLAR COUPLING

There are three main ways in which interchain-dipolar interactions can affect results and their interpretation. We discuss them here and make specific applications to CMC. They are (i) introduction of a nonsecular contribution to the relaxation function $\phi(t)$ when H_0 is along the chain axis, (ii) contribution of the isotropic part $g^2\mu_B^2 \vec{S}_i \cdot \vec{S}_j / r_{ij}^3$ to an effective interchain-exchange coupling for limiting one-dimensional diffusion, and (iii) effect on the Néel temperature. We find in all cases that such dipolar coupling is relatively unimportant compared with nearest-neighbor interchain exchange.

(i) The nonsecular part of the dipolar interaction comes from the terms giving rise to $M = \pm 1, \pm 2$ changes in the Zeeman quantum number. It does not produce an $e^{-t^{3/2}}$ decay of the relaxation function since the spin correlation functions are modulated by an $e^{iM\omega_0\tau}$ factor which guarantees convergence of $\int_0^\infty \psi_M(\tau)\,d\tau$, where $\psi_M(\tau)$ is the $M \neq 0$ contribution to $\psi(\tau)$. Hence we expect to find an exponential decay rate η_M resulting from ψ_M which should be given by

$$\eta_M = k\hbar M_2^{(M)}/J\,, \tag{50}$$

where $M_2^{(M)}$ is the second moment due to the $M \neq 0$ part of the dipolar interaction and k is a constant of the order of unity. The form of Eq. (50) is consistent with a decay of $\psi_M(\tau)$ in a characteristic time $1/\omega_e$ of the order of $\hbar/J$. It is also assumed that $\omega_0 \ll \omega_e$, so that η_M is essentially independent of ω_0. This is fairly well satisfied in the compounds studied here. The second moment $M_2^{(M)}$ is given by

$$M_2^{(M)} = \tfrac{3}{4}\gamma_e^4\hbar^2 S(S+1) \times \sum_j r_{ij}^{-6}\left(\sin^4\theta_{ij} + 10\sin^2\theta_{ij}\cos^2\theta_{ij}\right), \tag{51}$$

where we have combined all the $M \neq 0$ terms into one expression.

It is evident that $M_2^{(M)} = 0$ for a true linear chain when H_0 is along the chain axis. For a material such as CMC, however, $M_2^{(M)}$ can be appreciable even at $\theta = 0$ because of non-negligible interchain dipolar coupling. We have calculated the ratio

$$M_2^{(0)}/M_2^{(M)} = 4.1 \tag{52}$$

for CMC at $\theta = 0$, where $M_2^{(0)}$ is the secular part of the dipolar second moment, which is given by Eq. (51) with the quantity in parentheses replaced by $(3\cos^2\theta_{ij} - 1)^2$.

Uncertainty as to the constant k makes it somewhat difficult to give a reliable calculation of η_M starting from Eq. (1). Rather, we choose to estimate it by a simple scaling argument based on comparison with the situation in TMMC. The reasoning is as follows.

The one-dimensional relaxation rate γ is given by

$$\gamma = k'[M_2^{(0)}]^{2/3}/(J/\hbar)^{1/3} \tag{53}$$

and thus we expect to find, for TMMC,

$$\frac{\gamma(\theta=0)}{\eta_M(\theta=55^\circ)} = \frac{k'}{k}\ \frac{3}{2}\ \frac{J^{2/3}}{[M_2^{(0)}]^{1/3}}\ , \tag{54}$$

where the factor $\frac{3}{2}$ results from the ratio of $M_2^{(0)}$ at $\theta = 0$ and $M_2^{(M)}$ at $\theta = 55^\circ$, namely,

$$(3\cos^2\theta - 1)^2\big|_{\theta=0}/(10\sin^2\theta\cos^2\theta + \sin^4\theta)\big|_{\theta=55^\circ} = \tfrac{3}{2}\ .$$

Since $M_2^{(0)}$ is proportional to c^{-6} and since the spin values are the same for CMC and TMMC, the scaling relation is

$$\frac{(\gamma/\eta)_{\rm CMC}}{[\gamma(\theta=0)/\eta_M(\theta=55^\circ)]_{\rm TMMC}} = \tfrac{2}{3}\,4.1(J_{\rm CMC}/J_{\rm TMMC})^{2/3}\left(\frac{4.53}{3.25}\right)^2\ , \tag{55}$$

where we have used Eq. (52) and the ratio 4.53/3.25 between intrachain distances in CMC and TMMC. The experimental value $[\gamma(\theta=0)/\eta_M(\theta=55^\circ)]_{\rm TMMC} = 4.7$ is obtained from the literature[6] upon accounting for the relation Eq. (49) between γ and ΔH for an $e^{-(\gamma t)^{3/2}}$ relaxation function. We take $J_{\rm CMC}/J_{\rm TMMC} \approx \frac{3}{7}$ for the ratio between exchange constants[3,4,11] and thus arrive at

$$\gamma/\eta \approx 14 \quad \text{for CMC at } \theta = 0\ .$$

The relaxation function calculated in Sec. III B should then be multiplied by $e^{-\eta t}$ to account for the nonsecular terms. We have calculated the line shape in CMC at $\theta = 0$ with this factor included for $\eta = \frac{1}{14}\gamma$ and find that there is negligible effect in the range of experimental data.

There is a non-negligible effect at $\theta = \cos^{-1}(1/\sqrt{3})$ where the interchain-dipolar coupling can produce a nonzero secular term, as is evident from Eq. (34). The same scaling argument as used above then predicts $\gamma/\eta \approx 1$ for CMC in this case. There is then a slight non-Lorentzian character to the line even at the magic angle, which is shown by the dashed curve in Fig. 9.

(ii) Since there is an isotropic part

$$\mathcal{H}_{d,\,\rm exch} = \tfrac{1}{2}g^2\mu_B^2 \sum_{ij} r_{ij}^{-3}\vec{S}_i\cdot\vec{S}_j \tag{56}$$

of the dipolar Hamiltonian, it can give rise to effective values of J_1 and J_2 to be used in the formula of Sec. III. We estimate the size of these terms by noting from Eq. (26) that an interchain interaction G_{ij} enters into the expressions as

$$N^{-1}\sum_{q'} |G_{q'} - G_{q',-q}|^2 = 2\sum_j |G_{ij}|^2(1-\cos\vec{q}\cdot\vec{r}_{ij})\ , \tag{57}$$

where we have assumed inversion symmetry. Since we are interested only in that part of G_{ij} which produces variations in directions perpendicular to the chain, we take $q_z = 0$ and, further, consider only interactions with the chains at $x = \pm a$ and $y = \pm b$. Thence the effective dipolar contributions to interchain coupling are

$$J_{1d} = \tfrac{1}{2}g^2\mu_B^2\left[\sum_{n=-\infty}^{\infty}(n^2c^2 + a^2)^{-3}\right]^{1/2}\ , \tag{58a}$$

$$J_{2d} = \tfrac{1}{2}g^2\mu_B^2\left[\sum_{n=-\infty}^{\infty}(n^2c^2 + b^2)^{-3}\right]^{1/2}\ , \tag{58b}$$

where the additional subscript "d" indicates dipolar. Evaluation of the summations for CMC yields

$$J_{1d} = 2.0\times10^{-3}J\ , \tag{59a}$$

$$J_{2d} = 1.1\times10^{-3}J \tag{59b}$$

for $J/k_B = 3.0$ K. These values are close to an order of magnitude smaller than what are required to explain the observed line shape in CMC (Sec. VII).

We have also examined the effect of dipolar coupling on the interchain-exchange constants as determined by Skalyo *et al.*[38] from the spin-wave spectrum. Here we use previously derived formulas[40] to calculate $E_Q - E_0$, where E_Q is the spin-wave energy at the zone-boundary wave vector $(\pi/a,\ \pi/b,\ 0)$ and E_0 is the energy at zero wave vector.

We find that the observed $E_Q - E_0$ is too large to be explained by dipolar interactions alone and that the value of $J_1 + J_2$ (our notation) quoted by Skalyo *et al.* is not significantly altered, where J_1 and J_2 are taken to be nondipolar in origin. Note that lattice sums of the form

$$\textstyle\sum_j r_{ij}^{-3}(3\cos^2\theta_{ij} - 1)\,e^{i\vec{Q}\cdot\vec{r}_{ij}}\ ,$$

rather than the type given in Eqs. (58), are required for computation of E_Q.

(iii) Dipole interactions can also contribute toward stablizing long-range order and thus affect the Néel temperature. One way to estimate this effect is to compute the mean field experienced by a spin due to interchain-dipole interactions and compare it with that due to nearest-neighbor interchain-exchange interactions. For the antiferromagnetic state found by Skalyo *et al.* and by Spence *et al.*[35] we calculate $H_d'/H_E \ll 1$, where H_d' is the mean-interchain-dipolar field and H_E is the

exchange field. The fact that H_d' is so small may be seen at once from the spin alignment[35,38] since the fields from antiparallel neighbors at a distance of 7.285 Å, for which $\vec{S}_j$ and $\vec{r}_{ij}$ are antiparallel, nearly cancels that from antiparallel neighbors at a distance of 5.728 Å, for which $\vec{S}_j$ and $\vec{r}_{ij}$ are perpendicular $[2/(7.285)^3 \approx 1/(5.728)^3]$.

On this basis we then do not expect the dipolar interaction to influence the Néel temperature significantly. Other interactions, such as single-ion anisotropy, could of course play a more important role. Because of this, a certain amount of caution has to be exercised in inferring values of interchain-exchange constants from the Néel temperature.

VII. EXPERIMENTAL METHODS

Measurements of ESR absorption χ'' were made with an X-band microwave spectrometer operating at 8.68 GHz at room temperature. Straight dc detection was used (i.e., χ'' was detected directly rather than its derivative) with the klystron frequency tightly locked to the sample cavity.

Since we wished to study χ'' far from the line center (measurements are reported here for $|H - H_0| \lesssim 14\Delta H_{1/2}$), base-line drifts, dispersive components of the signal, and impurity resonances had to be carefully considered and eliminated. Drifts were minimized by signal averaging with a Fabritek model No. 1062 1024-channel analyzer. Signal averaging, of course, also allowed us to enhance signal-to-noise ratio, which was necessary for small samples far from the line center.

If the klystron frequency is well locked to the sample cavity, then only χ'' (i.e., the resistive component) should influence changes in reflection from the cavity. However, there is a secondary effect produced by the dispersive component χ' in that it changes the frequency. This can lead to undesirable changes in the reflection coefficient if the over-all microwave circuit is not sufficiently broadband. To overcome the problem, we used a directional coupler, rather than a bridge, to monitor reflected power and placed adjustable tuning screws near (less than $\frac{1}{4}$ of a guide wavelength) both the cavity iris and the directional coupler. In this way a broad-band circuit was attained whose center frequency coincided with the klystron frequency on magnetic resonance.

Resonances associated with impurities in the cavity walls presented an initial difficulty, but they were eliminated by silver plating the cavity. Silver plating also had the desirable effect of producing a high unloaded $Q_0 = 4000$ which led to good lock-in characteristics.

With these precautions, we were able to obtain symmetric absorption curves with no observable slope or other distortion of the baseline. Typical signal-averaged traces from which data are presented in the following Sec. VIII are shown in Fig. 7.

The symmetrical absorption curves obtained by sweeping the magnetic field indicate that Bloch's equations are incorrect even when the material has a Lorentzian line shape. These equations predict that the absorption is proportional to the bulk magnetization M_z, which is proportional to the applied magnetic field in the paramagnetic regime. This would lead to an asymmetrical absorption which is not observed in the experiment even out to

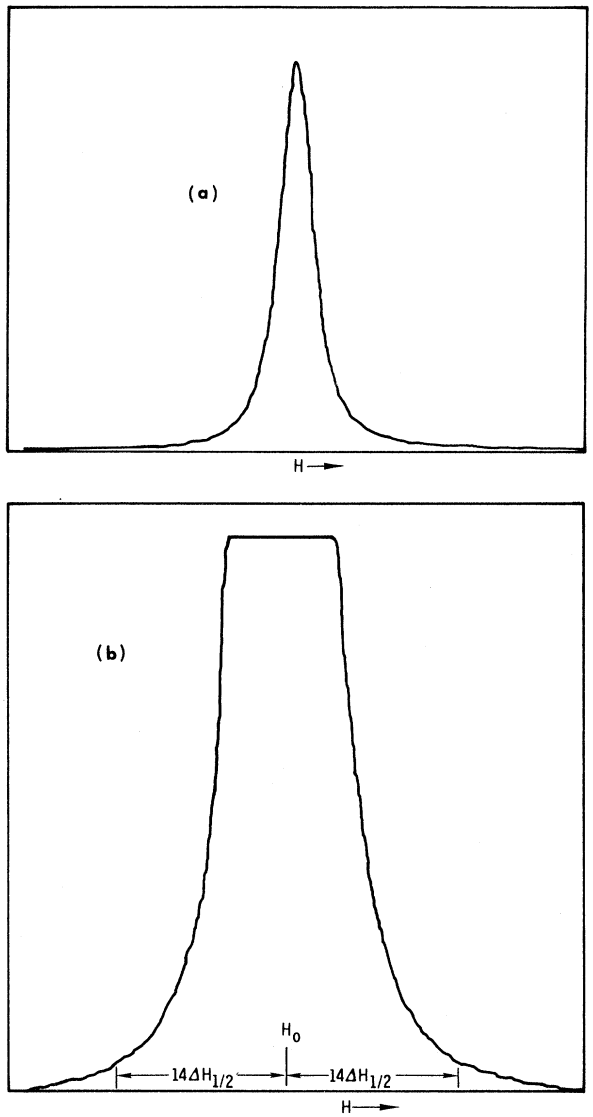

FIG. 7. Experimental line shapes in CMC with H along c axis. Shown are chart recorder outputs from memory of Fabritek model No. 1062 1024-channel analyzer. In curve (b) the gain is 16 times that of curve (a). For each the total sweep is 5850 Oe. Curve (a) is subject to nonlinearities, and direct measurements are not made from it.

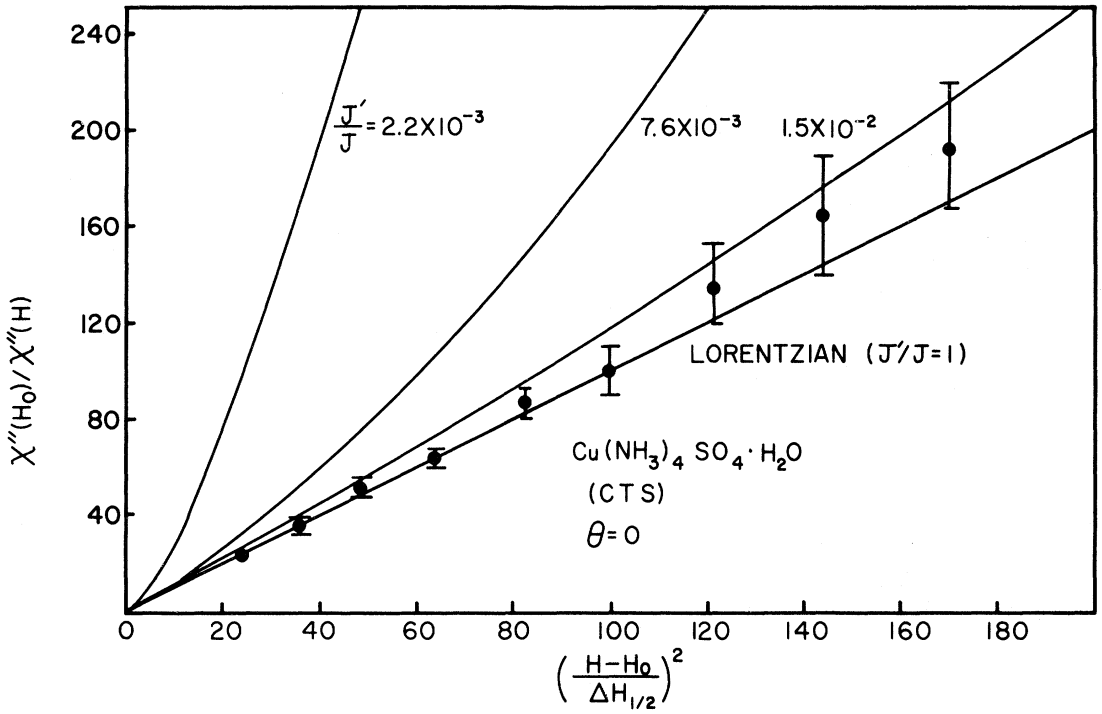

FIG. 8. Line shape for CTS. Room-temperature 8.68-GHz field along chain axis ($\theta=0$). Experimental linewidth is $2\Delta H_{1/2}=40$ Oe. Points are average between high-field ($H-H_0>0$) and low-field ($H-H_0<0$) values, and error bars represent difference between high- and low-field measurements. Theoretical curves are for values of J'/J shown in Table I. The resulting theoretical linewidths are given in Table II.

$\pm 20\Delta H_{1/2}$. Instead we find that the absorption is proportional to the microwave frequency and line-shape function, which is consistent with the quantum-mechanical picture of absorption, Eq. (1), and with the results of low-frequency-susceptibility measurements in zero magnetic field. The fact that Bloch's equations fail to give an adequate description of the absorption for a Lorentzian line shape has been discussed earlier by Garstens.[41] However, this is, to our knowledge, the first observation of the effect far out in the wings of the absorption.

VIII. RESULTS AND COMPARISON WITH THEORY

A. CTS

Single crystals of CTS were grown from solutions by dissolving $CuSO_4\cdot 2H_2O$ in an excess of NH_4OH as described by Abe and Ono.[42] The room-temperature width at 8.68 GHz with H parallel to the chain axis was $2\Delta H_{1/2}=40$–45 Oe, for a variety of samples, in reasonable agreement with previously reported measurements.[42–44] In Fig. 8, we show the line shape out to $14\Delta H_{1/2}$. The function $\chi''(H)$ is plotted vs $[(H-H_0)/\Delta H_{1/2}]^2$ (H_0 is the value of the field H on resonance), since this yields a straight line for a Lorentzian line shape. A non-resonant term $[(H+H_0)/\Delta H_{1/2}]^2$ need not be included since it gives less than a 1% effect even at $14\Delta H_{1/2}$. The data show at most only a slight deviation from a Lorentzian curve. As shown, they are in accord with the theory of Sec. III for $J_1/J=1.5\times10^{-2}$, the Tahir-Kheli (TK) estimate (see Table I), but not for the RPA value of $J_1/J=7.6\times10^{-3}$. We have taken $2\Delta\tilde{H}_{1/2}=75$ Oe for the one-dimensional linewidth, as discussed in Sec. V A.

B. CMC

Single crystals of CMC were grown from aqueous solution as described in Ref. 11. The room-temperature width at 8.68 GHz with H parallel to the chain axis was $2\Delta H_{1/2}=232$ Oe, in agreement with published data.[45] The line shape is non-Lorentzian for H along the chain axis, as shown in Fig. 9, but, as expected,[8] is nearly Lorentzian for H 54° from the chain axis ($3\cos^2\theta-1=0$). These line-shape and linewidth data are in accord with independent measurements by Ajiro *et al.*[46] Lorentzian shapes were reported in Ref. 44, but it is evident from Fig. 9 that unless observations extend out to about ten half-widths, the non-Lorentzian character will not be seen.

From the observed Néel temperature and J (Table I), we obtain

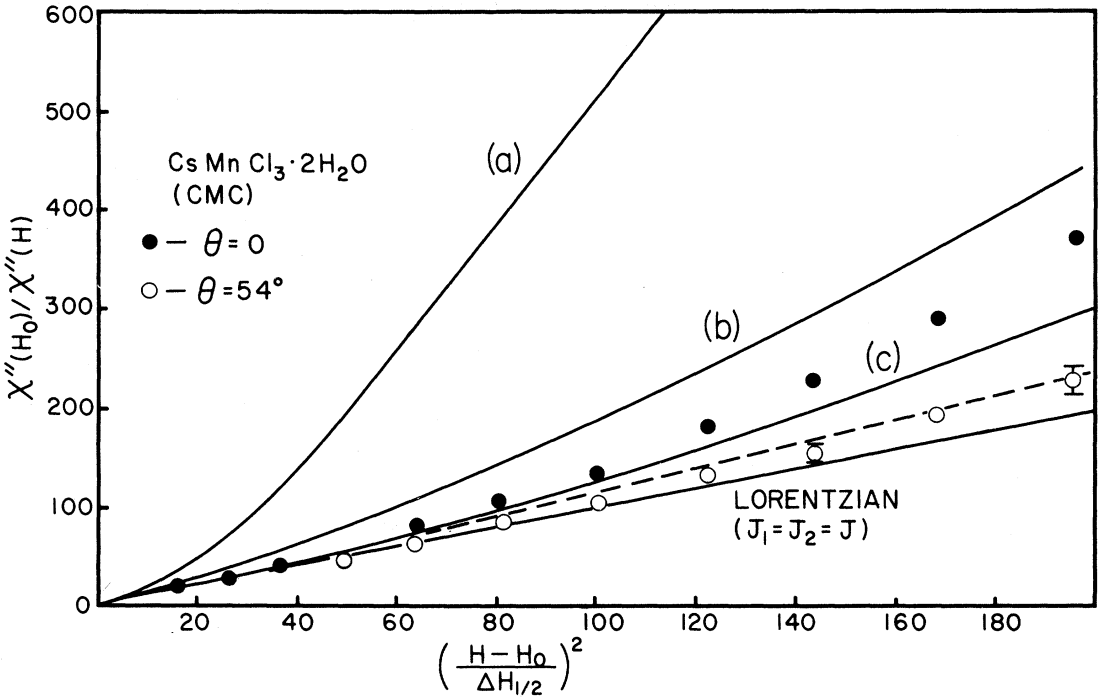

FIG. 9. Line shape for CMC. Room-temperature 8.68-GHz field along chain axis ($\theta = 0$) and at 54° from axis. Experimental linewidth is $2\Delta H_{1/2} = 232$ Oe for $\theta = 0$. Differences between $H - H_0 > 0$ and $H - H_0 < 0$ points are smaller than drawn circles, except where indicated by error bars. Solid-theoretical curves for $\theta = 0$ are (a) $J_1 = J_2 = 6 \times 10^{-3}\ J$, which gives $2\Delta H_{1/2} = 370$ Oe; (b) $J_1 = 100\ J_2 = 2.6 \times 10^{-2} J$, which gives $2\Delta H_{1/2} = 240$ Oe; (c) $J_1 = J_2 = 2 \times 10^{-2} J$, which gives $2\Delta H_{1/2} = 210$ Oe. Dashed curve is theoretical for $\theta = 54°$ including a one-dimensional contribution $\gamma = \eta$ due to interchain-dipolar coupling (Sec. VI). Linewidth values for (a), (b), (c) are based on one-dimensional value $2\Delta\tilde{H}_{1/2} = 490$ Oe.

$$J_1/J = 5.8 \times 10^{-3}[1 + 0.245 \ln(J_1/J_2)]^2 \ . \qquad (60)$$

Theoretical curves are presented in Fig. 9 for two values of J_1/J which satisfy Eq. (60), corresponding to $J_1 = J_2$ and to $J_1 = 100 J_2$. We have added the dipolar contributions Eq. (59) to these values. The only important influence of the dipolar term comes from J_{2d} for the case $J_1 = 100\ J_2$. Also shown is the line shape for $J_1 = J_2 = 0.02\ J$.

The line shape does not depart from Lorentzian as much as would be indicated either from the Néel temperature estimate of J_1 and J_2 or from the neutron data of Skalyo *et al.* The value of $J_1 + J_2$ needed to describe the line shape is about a factor of 4 larger than measured from the spin-wave spectrum.[38]

There is a good agreement for the absolute width in the sense that the J_1 and J_2 required to give the observed line shape also yield a value of $2\Delta H_{1/2}$ close to the measured 232 Oe, when we use $2\Delta\tilde{H}_{1/2} = 490$ Oe, the result (Sec. V B) obtained from scaling with TMMC.

The dashed curve in Fig. 9 is the predicted line shape at $\theta = 54°$ when a finite γ due to interchain-dipolar interactions is included, as discussed in Sec. VI. It shows a slight departure from Lorentzian, in accord with the data, but the deviation from Lorentzian is only about 20% at 14 half-widths and thus not important.

C. CuPC

Small needlelike crystals were grown as described in Ref. 15. In order to obtain sufficient signal strength, it was convenient to use a bundle of crystals with a common needle axis. X-ray diffraction verified that the needle axis coincides with the chain c axis. Thus all the chain axes were parallel and meaningful measurements could be performed with the field along the c axis. Anisotropy of the g tensor, however, complicates measurements with H away from the chain axis. Figure 10 shows the line shape for CuPC at room temperature. The line is highly non-Lorentzian for H along the chain axis ($\theta = 0$). For comparison, we also show data at $\theta = 90°$ which, as expected,[8] has less departure from Lorentzian. At $\theta = 54°$ there was considerable structure in the line, presumably due to the multicrystals, and it was not possible to obtain a meaningful line shape.

The data are used to estimate T_N for CuPC as follows. The observed values $2\Delta H_{1/2} = 53$ Oe and $\chi''(H_0)/\chi''(H)$ lead to a given number for J_1/J for

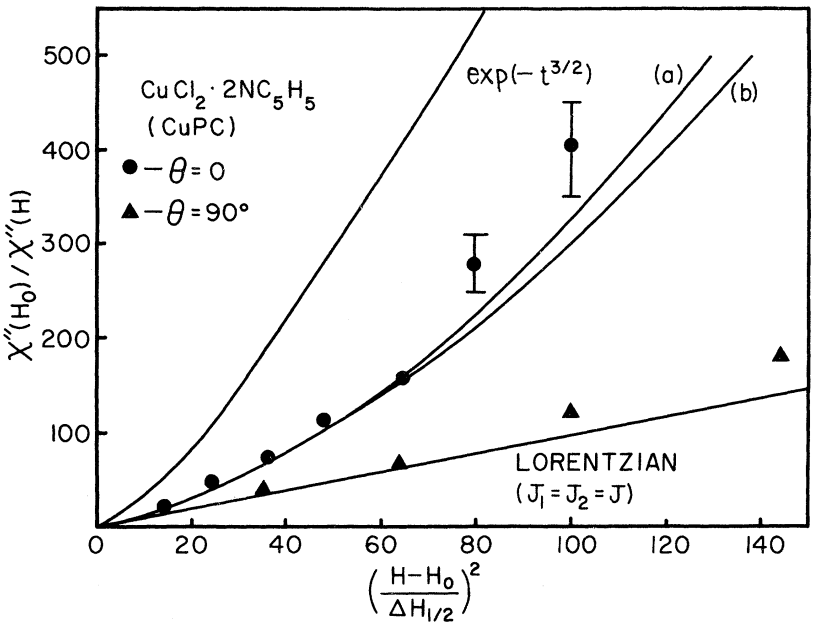

FIG. 10. Line shape for CuPC. Room-temperature 8.68-GHz field at $\theta = 0$ and 90° with respect to chain axis. Experimental linewidth is $2\Delta H_{1/2} = 53$ Oe at $\theta = 0$. Points are for $H < H_0$. The high-field ($H > H_0$) line shape was somewhat irregular due to the bundle of crystallites used. The curve labeled $\exp(-t^{3/2})$ is the pure one-dimensional line shape. Curves (a) and (b) are (a) $J_1 = J_2 = 1.8 \times 10^{-3} J$, (b) $J_1 = 10\, J_2 = 2.9 \times 10^{-3} J$, and are based on a one-dimensional linewidth $2\Delta\tilde{H}_{1/2} = 77$ Oe.

a particular ratio of J_1/J_2, upon application of the theory of Sec. III. Once estimates are made for J_1/J and J_1/J_2, the Néel temperature is given by the theory of Sec. IV. Our numerical method is shown in Fig. 11, where $\chi''(H_0)/\chi''(H)$ at $H - H_0 = 10\Delta H_{1/2}$ is plotted vs J_1/J for several values of J_1/J_2. We can then pick the proper J_1/J for a given J_1/J_2 which gives close to the observed amplitude at $10\Delta H_{1/2}$. Note that the curves are insensitive to J_1/J_2 for $J_1/J_2 \gtrsim 2$. As a consequence, we can give a reasonable estimate for J_1/J without knowing T_N or the value of J_1/J_2. The physical reason for this is that the line shape is insensitive to J_2 for $\gamma t_2 \gg 1$, where $t_2 \approx (J_1/J_2)^{4/3} t_0$ is the characteristic time at which interchain motion in the y direction (Fig. 1) becomes important. Once values for J_1 and J_2 are selected from curves such as given in Fig. 11, the entire theoretical line shape may be plotted. Two such curves are shown in Fig. 10, corresponding to $J_1/J_2 = 1$ and to $J_1/J_2 = 10$. As mentioned in Sec. V C, the crystal structure makes it likely that J_1/J_2 lies between these two values.

For the numbers found ($J_1/J = 1.9 \times 10^{-3}$, J_1/J_2

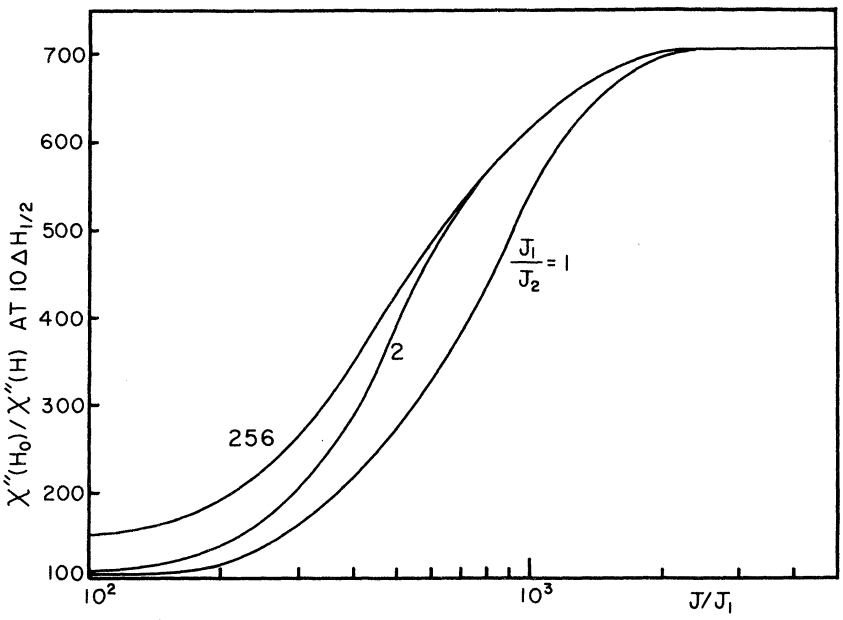

FIG. 11. Theoretical line shape at $10\Delta H_{1/2}$ vs J/J_1. Values are for CuPC with $2\Delta\tilde{H}_{1/2} = 77$ Oe.

TABLE III. Parameters obtained for CuPC from observed line shape (Fig. 10) and experimental value $2\Delta H_{1/2}=53$ Oe. Tahir-Kheli (TK), RPA, and Callen (C) methods are used to predict T_N from J_1 and J_2. Measured value Ref. 39 is $T_N=1.135$ K.

CuPC	$2\Delta\tilde{H}_{1/2}$	J_1/J	T_N (TK)	T_N (RPA)	T_N (C)
$J_1=J_2$	77 Oe	1.9×10^{-3}	0.61 K	0.92 K	1.83 K
$J_1=10J_2$	77 Oe	2.9×10^{-3}	0.48 K	0.73 K	1.44 K

$=1$; $J_1/J=2.9\times10^{-3}$, $J_1/J_2=10$), Eqs. (40) and (44) can be used to predict T_N in the various schemes. Results, which are contained in Table III, show that a value of f intermediate between the RPA and the Callen values can account for the recently observed[39] $T_N=1.135$ K. As mentioned in Sec. V C, the analysis was performed before we were aware of the measurement of T_N. It has been retained in the form of a prediction for T_N since it shows in principle how one might be able to estimate the transition temperature from an observed ESR line shape.

Both curves through the data in Fig. 10 correspond to $2\Delta\tilde{H}_{1/2}=77$ Oe, which is in excellent agreement with the estimate (Sec. V C) of 80 Oe based on scaling with CuNSAL.

IX. SUMMARY AND CONCLUSIONS

We have developed a theory for the effect of weak interchain couplings on the ESR line shape in Heisenberg linear chains. It has then been compared with our experimental line shapes in three compounds: $Cu(NH_3)_4SO_4\cdot H_2O$ (copper tetramine sulfate monohydrate, referred to as CTS), $CsMnCl_3\cdot 2H_2O$ (cesium manganese chloride dihydrate, referred to as CMC), and $CuCl_2\cdot 2NC_5H_5$ [dichloro*bis*-(pyridine)-copper (II), referred to as CuPC].

The main result of the theory is that the characteristic time t_0 at which interchain spin flips become important is of the order of $\hbar[J'(J'/J)^{1/3}]^{-1}$. The factor $(J'/J)^{1/3}$ occurs because the effective rate at which off-chain motion is interrupted is small because of the slow $t^{-1/2}$ decay of spin correlations by intrachain diffusion. If the on-chain correlations decayed rapidly enough to give a finite zero-frequency component (a $t^{-1/2}$ decay produces an $\omega^{-1/2}$ divergence as frequency $\omega\to0$), then the factor would be (J'/J), as consistent with simple Golden Rule and analysis-of-moments arguments.

The line shape may be computed numerically once the interchain coupling is known; and this coupling has been estimated from the observed Néel temperatures using RPA and other Green's-function decoupling schemes. Unequal interchain couplings J_1 and J_2 for an orthorhombic lattice have been treated.

Experimental data show a Lorentzian line in CTS, which is consistent with theory if the Tahir-Kheli (TK) scheme for estimating J'/J is used. The non-Lorentzian line in CMC agrees with theory only for $J_1/J_2\approx100$. A difference between J_1 and J_2 is to be expected for the orthorhombic crystal structure of CMC, but $J_1/J_2\approx10$ seems to be more reasonable. Since the transition temperature T_N was not known for CuPC during this work, we could not compare the non-Lorentzian line with theoretical estimates. Instead, we used the observed departure from Lorentzian to estimate the interchain coupling and thereby gave predictions for T_N. The newly found value $T_N=1.135$ K lies between our estimates based on the RPA and the Callen schemes, but is about a factor of 2 larger than predicted by the TK method.

We conclude that the theory presented here can explain at least the qualitative features of our data, particularly the Lorentzian line in CTS. It is not clear whether we can fully account for the effectiveness of interchain coupling since the values for J_1 and J_2 in CMC are about a factor of 4 larger than indicated by neutron measurements of the spin-wave spectrum and about a factor of 2 larger than indicated from the Néel temperature. Temperature dependence of the parameters could be playing a role since our measurements are at room temperature while the other data are in or near the liquid-helium range. However, uncertainty about approximations both in the theory of the transition temperature and in the theory of interchain effects on line shape makes it risky to assume quantitative accuracy to within better than, say, a factor of 2. It does seem possible, though, to assert that the basic relation $t_0^{-1}\propto J'(J'/J)^{1/3}$ is correct, since the Golden Rule result $t_0^{-1}\propto J'(J'/J)$ would predict line shapes to be very nearly pure one dimensional for any of the parameters used in Figs. 8–10.

Comments are in order regarding effects other than interchain coupling. Spin-lattice relaxation, for example, is an alternate means whereby the $t^{-1/2}$ decay of the correlations could be damped out. The argument against this is that a spin-lattice relaxation rate Γ must contribute an amount Γ/γ_e to the observed width in Oe. Thus, we must always have $\gamma_e\Delta H_{1/2}\geq\Gamma$; but from Table II we see that $\gamma_e\Delta H_{1/2}<t_0^{-1}$ is required for agreement with experiment. Hence, the characteristic interchain time t_0 is less than any spin-lattice relaxation time. Furthermore, it is likely for the Kramers ions considered here that t_0 is at least an order of magnitude smaller than the spin-lattice relaxation time. Note also that $\gamma_e\Delta H_{1/2}=\Gamma$ would imply that all the observed width is associated with spin-lattice relaxation which hardly seems reasonable for the temperature-independent (at high temperature), strongly dipole-coupled widths observed in these

materials. Similar arguments prevail against other "randomizing" mechanisms such as proposed by Soos.[47] Any such mechanism with a characteristic rate Γ' should contribute an amount Γ'/γ_e to $\Delta H_{1/2}$, *unless* it comes from a Hamiltonian which commutes with the total spin. Isotropic-interchain coupling is such a Hamiltonian, and therefore, it can produce a rate t_0^{-1} such that $\gamma_e \Delta H_{1/2} < t_0^{-1}$. It is difficult to envisage any other mechanism which can do this.

Our model has been based strictly on isotropic nearest-neighbor interchain couplings J_1 and J_2. In general, interchain-dipolar couplings can be important and lead to different values for effective interchain-coupling constants. We have treated this in some detail for CMC, however, and find that the dipolar effects for the most part are negligible.

ACKNOWLEDGMENTS

Dr. B. Morosin aided in preparation of the samples, performed x-ray analysis, and provided helpful insights into the structures of the compounds studied here. Professor W. Duffy, Jr. kindly allowed us to quote his datum on T_N for CuPC prior to its publication. We have also profited from discussions and communications with Dr. R. R. Bartkowski, Professor J. W. Culvahouse, Professor S. A. Friedberg, Professor Z. G. Soos, and Professor W. P. Unruh.

APPENDIX: VALIDITY OF EQ. (22) TO ORDER t^2

Consider

$$\left|\frac{d^2}{dt^2}\,\langle \tilde{S}_q^z(t)\bar{S}_{-q}^z(-t)\rangle\right|_{t=0}$$

$$= \langle \ddot{\tilde{S}}_q^z S_{-q}^z\rangle + \langle S_q^z \ddot{\bar{S}}_{-q}^z\rangle + 2\,\langle \dot{\tilde{S}}_q^z \dot{\bar{S}}_{-q}^z\rangle\,, \quad \text{(A1)}$$

where dots $(\cdot)$ represent time differentiation and quantities are evaluated at $t=0$. Similarly, we have

$$\left|\frac{d^2}{dt^2}\,\langle S_q^z(0)\bar{S}_{-q}^z(-t)\rangle\,\tilde{\phi}_q(t)\right|_{t=0}$$

$$= \langle S_q^z S_{-q}^z\rangle\,\ddot{\tilde{\varphi}}_q + \langle S_q^z \ddot{\bar{S}}_{-q}^z\rangle + 2\,\langle S_q^z \dot{\bar{S}}_{-q}^z\rangle\,\dot{\tilde{\phi}}_q\,. \quad \text{(A2)}$$

It follows from Eq. (21) that the first terms on the right-hand sides of (A1) and (A2) are equal. The quantity $\dot{\tilde{\varphi}}_q$ is given by

$$\dot{\tilde{\phi}}_q = (1/\hbar)\,\langle [\mathcal{H}_I\,, S_q^z]\,S_{-q}^z\rangle / \langle S_q^z S_{-q}^z\rangle \quad \text{(A3)}$$

and is zero as long as static off-chain correlations may be neglected. This is because $[\mathcal{H}_I\,, S_q^z]S_{-q}^z$ involves products of three-spin operators, at least two of which must belong to different chains, because of the interchain nature of $\mathcal{H}_I$. Since off-chain static correlations are of the order of J'/k_BT, we find that the third term on the right-hand side of (A2) is of the order of $J\times J'\times(J'/k_BT)$, whereas the first term is of the order $(J')^2$. Thus the third and first terms are in the ratio J/k_BT. Similarly, the term $\langle \dot{\tilde{S}}_q^z \dot{\bar{S}}_{-q}^z\rangle$ is of the order of $J\times J'\times(J'/k_BT)$ since it also is zero unless static off-chain correlations are included. (This is because $\dot{\tilde{S}}_q^z$ contains two-spin operators which are on different chains while $\dot{\bar{S}}_{-q}^z$ has two-spin operators which belong to the same chain.) Thus, we find that the third terms on the right-hand sides of (A1) and (A2) are negligible in the high-temperature limit, $J/k_BT \ll 1$. Since the first two terms are equal, this establishes validity of Eq. (22) to order t^2.

---

*Work supported by the U. S. Army Research Office, Durham and by the U. S. Atomic Energy Commission. Preliminary accounts of portions of this work have appeared in Bull. Am. Phys. Soc. 15, 269 (1970); 16, 380 (1971).

†Present address: Texaco Inc., Bellaire, Tex. 77401.

‡Present address: Sandia Laboratories, Albuquerque, N. M.

[1]H. A. Bethe, Z. Physik 21, 205 (1931).

[2]R. Dingle, M. E. Lines, and S. L. Holt, Phys. Rev. 187, 643 (1969).

[3]R. J. Birgeneau, R. Dingle, M. T. Hutchings, G. Shirane, and S. L. Holt, Phys. Rev. Letters 26, 718 (1971).

[4]M. T. Hutchings, G. Shirane, R. J. Birgeneau, and S. L. Holt, Phys. Rev. B 5, 1999 (1972).

[5]R. Kubo and K. Tomita, J. Phys. Soc. Japan 9, 888 (1954).

[6]H. Mori and K. Kawasaki, Progr. Theoret. Phys. (Kyoto) 27, 529 (1962).

[7]General treatment of line shapes may also be found in the texts, A. Abragam, *Principles of Nuclear Magnetism* (Oxford U. P., New York, 1961); C. P. Slichter, *Principles of Magnetic Resonance* (Harper and Row, New York, 1963).

[8]R. E. Dietz, F. R. Merritt, R. Dingle, D. Hone, B. G. Silbernagle, and P. M. Richards, Phys. Rev. Letters 26, 1186 (1971).

[9]R. R. Bartkowski, M. J. Hennessy, B. Morosin, and P. M. Richards, Solid State Commun. 11, 405 (1972).

[10]R. B. Griffiths, Phys. Rev. 135, A659 (1964).

[11]T. Smith and S. A. Friedberg, Phys. Rev. 176, 660 (1968).

[12]K. Takeda, S. Matsukawa, and T. Haseda, J. Phys. Soc. Japan 30, 1330 (1971).

[13]C. D. McElwee, thesis (University of Kansas, 1970) (unpublished).

[14]P. M. Richards, in Proceedings of the Midwinter Solid State Research Conference, Newport Beach, Calif., 1972 (unpublished).

[15]D. Hone, in *AIP Conference Proceedings, Magnetism and Magnetic Materials*, No. 5, 1971, edited by C. D. Graham, Jr. and J. J. Rhyne (AIP, New York, 1972), p. 413.

[16]P. G. de Gennes, J. Phys. Chem. Solids 4, 223 (1958).

[17]H. S. Bennett and P. C. Martin, Phys. Rev. 138, A608 (1965).
[18]R. A. Tahir-Kheli and D. G. McFadden, Phys. Rev. 182, 604 (1969).
[19]J. E. Gulley, D. Hone, D. J. Scalapino, and B. G. Silbernagle, Phys. Rev. B 1, 1020 (1970).
[20]S. J. Jensen, P. Anderson, and S. E. Rasmussen, Acta. Chem. Scand. 16, 1890 (1962).
[21]F. Mazzi, Acta. Cryst. 8, 137 (1955).
[22]B. Morosin, Acta. Cryst. B 25, 19 (1969).
[23]M. F. Collins and W. Marshall, Proc. Phys. Soc. (London) 92, 390 (1967).
[24]G. N. Watson, *A Treatise on the Theory of Bessel Functions* (Cambridge U. P., New York, 1962), p. 203.
[25]H. B. Callen, Phys. Rev. 130, 890 (1963).
[26]R. A. Tahir-Kheli, Phys. Rev. 132, 689 (1963); see also R. H. Swendson, Phys. Rev. B 5, 116 (1972).
[27]G. S. Rushbrooke and P. J. Wook, Mol. Phys. 6, 409 (1963).
[28]E. Montroll, *Proceedings of the 3rd Berkeley Symposium on Mathematical Statistics and Probability* (University of California Press, Berkeley, 1956), Vol. III.
[29]T. Oguchi, Phys. Rev. 133, A1098 (1964).
[30]T. Haseda and A. R. Miedema, Physica 27, 1102 (1961).
[31]T. Watanabe and T. Haseda, J. Chem. Phys. 29, 1492 (1958).
[32]S. Saito, J. Phys. Soc. Japan 26, 1388 (1969).
[33]R. N. Rogers (private communication).
[34]M. E. Fisher, Am. J. Phys. 32, 343 (1964).
[35]R. D. Spence, W. J. M. de Jonge, and K. V. S. Rama Rao, J. Chem. Phys. 51, 4694 (1969).
[36]G. J. Butterworth and J. A. Wollam, Phys. Letters 29A, 259 (1969).
[37]D. Bloch, J. Phys. Chem. Solids 27, 881 (1966); D. H. Lowndes, Jr., L. Finegold, R. N. Rogers, and B. Morosin, Phys. Rev. 186, 515 (1969).
[38]J. Skalyo, Jr., G. Shirane, S. A. Friedberg, and H. Kobayashi, Phys. Rev. B 2, 4632 (1970).
[39]W. Duffy, Jr. (private communication).
[40]O. Nikotin, P. A. Lindgard, and O. W. Dietrich, J. Phys. C 2, 1168 (1969).
[41]M. A. Garstens, Phys. Rev. 93, 1228 (1954).
[42]H. Abe and K. Ono, J. Phys. Soc. Japan 11, 947 (1956).
[43]M. Date, J. Phys. Soc. Japan 11, 1016 (1956).
[44]S. Saito, Phys. Letters 24A, 442 (1967).
[45]Y. Tazuke and K. Nagata, J. Phys. Soc. Japan 30, 285 (1971). Their peak-to-peak derivative linewidths should be multipled by $\sqrt{3}$ to obtain $2\Delta H_{1/2}$ for a nearly Lorentzian line.
[46]Y. Ajiro, N. S. Vanderven, and S. A. Friedberg, in Ref. 15, p. 433; Y. Ajiro and S. A. Friedberg (private communication).
[47]Z. G. Soos, J. Chem. Phys. 44, 1729 (1966).

PHYSICAL REVIEW B VOLUME 7, NUMBER 3 1 FEBRUARY 1973

Isomer-Shift Calibrations Using Multivalent States of ^{57}Fe in $KMgF_3$ †

A. Trautwein*
Institut für Metallphysik, Universität des Saarlandes, 66 Saarbrücken, West Germany

and

J. R. Regnard
Centre d'Etudes Nucleaires, Grenoble, France

and

Frank E. Harris
Department of Physics, University of Utah, Salt Lake City, Utah 84112

and

Y. Maeda‡
Institut für Metallphysik, Universität des Saarlandes, 66 Saarbrücken, West Germany
(Received 14 July 1972)

$KMgF_3$ single crystals were doped with ^{57}Fe and irradiated by ^{60}Co γ rays. The obtained Fe^{+}, Fe^{++}, and Fe^{+++} states in $KMgF_3$ were investigated by Mössbauer spectroscopy. The isomer-shift values were correlated with electron densities $\rho(0)$ as evaluated by using an open-shell molecular-orbital procedure. The resulting isomer-shift calibration constant α is $(-0.34 \pm 0.04)\, a_0^3$ mm sec^{-1}.

I. INTRODUCTION

The Mössbauer isomer shift (IS) between two iron compounds is proportional to the difference of the electron densities $\Delta\delta(0)$ at the Mössbauer nuclei: $\Delta\delta = \alpha\Delta\rho(0)$. Knowing α one could derive electron densities directly from δ. There exist several theoretical approaches to derive $\rho(0)$, as reviewed by Kalvius.[1] In the present paper we use a spin-projected configuration-interaction method[2] followed by a renormalization procedure of the Fe 3*s* atomic orbital to evaluate $\rho(0)$. The investi-